ARCHIVES OF ACOUSTICS
9, 3, 305-316 (1984)

THE ACOUSTIC FIELD ON THE AXIS OF A CIRCULAR CONE

HENRYK TYGIELSKI, WITOLD RDZANEK

Department of Theoretical Physics, Higher Pedagogical School
(65–562 Zielona Góra, pl. Słowiański 6)

It was assumed in this paper that the sound source was placed on the surface of an ideal rigid circular cone. The vibration velocity amplitude at the source was constant. Solution of the wave equation in a system of spherical coordinates, by using the Kontorovich-Lebedev transformation, gave the acoustic potential. Expressions for the acoustic pressure on the axis of a circular cone were derived, and these calculations were represented graphically.

Notation

a, b – radial coordinates of the sound source
c – sound velocity
$H_\mu^{(2)}$ – cylindrical Hankel function of the μth order, of the second kind
J_μ – cylindrical Bessel function of the μth order
k – wave number
p – acoustic pressure
P_μ – Legendre function
r – coordinate in a spherical system
t – time
z – coordinate in a Cartesian system
v_0 – normal component of the vibration velocity amplitude on the surface of the source
β – conical angle (measured from the axis z to the surface of the cone)
θ – angular coordinate in a spherical system
μ – variable occurring in the Kontorovich-Lebedev transformation
ν_n – nth root of equation (20)
ϱ – density of the medium
Φ – acoustic potential
ω – angular frequency

1. Introduction

Vibrating planar, cylindrical or spherical surfaces are among the most frequent practical surface acoustic sources and the deeply investigated fields radiated by these sources.

There is less knowledge on the acoustic field distribution radiated by sources with more complex geometry, e.g. vibrating spheroidal or conical surfaces.

In paper [1] CARLISE considered a vibrating source element on a cone as a system of pairs of point sources. On the basis of the results obtained, he analysed the radiation conditions of a conical loudspeaker and gave experimental results.

The problems of the acoustic field of a source placed on a cone, the latter being in an ideal rigid and planar baffle, were considered in the papers of SLUSARENKO and DOBRUCKI [4, 14]. These authors, using the Rayleigh-Huygens integral, derived an expression for the acoustic pressure distribution. However, these results were approximate and can only be used in calculating pressures at a large distance from the source for some conical angles.

In his paper [15] TYGIELSKI considered the problem of the acoustic field of a source situated on the surface of an infinitely long, ideal rigid cone with circular termination. He solved the inhomogeneous equation for a Green function in a system of spherical coordinates. Integrating the Green function over the surface of the source, he obtained the acoustic potential. He also considered the case of the acoustic field at a large distance from the top of the cone.

The acoustic field of a point source close to an ideal rigid or an ideal compliant cone was analysed in the papers by CARSLAW [3], FELSEN [5, 6] and VAYSLEYB [16].

The present paper considered the problem of the acoustic field of a source situated on the surface of an ideal rigid, infinitely long circular cone. It was assumed that the normal component of the vibration velocity at the source was constant. Solution of the wave equation in a system of spherical coordinates, using the Kontorovich-Lebedev transformation, gave the acoustic potential. An expression was given for the acoustic pressure on the axis of the cone. Assumption that the conical angle was $\pi/2$ led to formulae representing the pressure on the axis of a source situated in an ideal rigid, planar baffle, which are known from the literature. These calculations were represented graphically.

The expressions derived in this paper can be used to calculate the acoustic pressure at any distance from the source, with conical angles from 0 to π.

2. Acoustic potential of the cone

On an ideal rigid, infinitely long conical baffle with a divergence angle β there is a surface sound source ($a \leqslant r \leqslant b$, $0 \leqslant \varphi < 2\pi$) with a uniform vibration velocity amplitude distribution (Fig. 1). The top of the cone is at the origin of the coordinate system. The radiation area is defined as follows: $0 \leqslant r < \infty$, $0 \leqslant \theta \leqslant \beta < \pi$, $0 \leqslant \varphi < 2\pi$.

The acoustic potential for the time dependence of the $\exp(i\omega t)$ type satisfies the wave equation

$$\Delta\Phi(\boldsymbol{r}) + k^2\Phi(\boldsymbol{r}) = 0, \tag{1}$$

where $\boldsymbol{r}$ – the tracing vector of the observation point, $k = \omega/c$ – the wave number. This equation is solved with the Neumann boundary condition. In

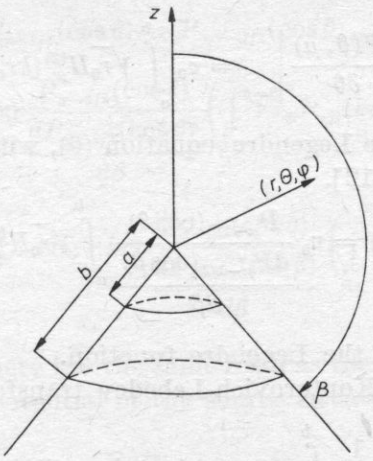

Fig. 1. The sound source on the surface of a revolution cone

view of the axial symmetry of the sound source, equation (1) can be written in a system of spherical coordinates

$$\frac{1}{r^2}\frac{\partial}{\partial r}\left(r^2\frac{\partial\Phi(r,\theta)}{\partial r}\right) + \frac{1}{r^2\sin\theta}\frac{\partial}{\partial\theta}\left(\sin\theta\frac{\partial\Phi(r,\theta)}{\partial\theta}\right) + k^2\Phi(r,\theta) = 0. \tag{2}$$

It is considered in the above equation that the acoustic potential does not depend on the angle variable φ. The Neumann boundary condition becomes

$$\left.\frac{1}{r}\frac{\partial\Phi(r,\theta)}{\partial\theta}\right|_{\theta=\beta} = \begin{cases} v_0 \text{ for the source,} \\ 0 \text{ beyond the source.} \end{cases} \tag{3}$$

In order to eliminate the variable r from equation (2), the following substitution can be used:

$$\Phi(r,\theta) = \frac{\Phi_0(r,\theta)}{\sqrt{r}}. \tag{4}$$

This substitution gives an equation in which the radial part of the Laplace operator occurs in a cylindrical coordinate system. Use of the Kontorovich-Lebedev transformation [9]

$$\Psi(\theta,\mu) = \int_0^\infty \Phi_0(r,\theta)\frac{H_\mu^{(2)}(kr)}{r}\,dr \tag{5}$$

and consideration that the Hankel function $H_\mu^{(2)}(kr)$ satisfies the Bessel equation [8, 12] lead to the equation with one independent variable θ

$$\frac{1}{\sin\theta}\frac{\partial}{\partial\theta}\left(\sin\theta\frac{\partial\Psi(\theta,\mu)}{\partial\theta}\right)+\left(\mu-\frac{1}{2}\right)\left(\mu+\frac{1}{2}\right)\Psi(\theta,\mu)=0. \tag{6}$$

The boundary condition (3), when considering transformation (5), becomes

$$\left.\frac{\partial\Psi(\theta,\mu)}{\partial\theta}\right|_{\theta=\beta}=v_0\int_a^b\sqrt{r_0}H_\mu^{(2)}(kr_0)\,dr_0. \tag{7}$$

The solution of the Legendre equation (6), with the boundary condition (7), is the function [7, 12].

$$\Psi(\theta,\mu)=v_0\frac{P_{\mu-1/2}(\cos\theta)}{\dfrac{dP_{\mu-1/2}(\cos\beta)}{d\beta}}\int_a^b\sqrt{r_0}H_\mu^{(2)}(kr_0)\,dr_0, \tag{8}$$

where $P_{\mu-1/2}$ represents the Legendre function.

Using the inverse Kontorovich-Lebedev transformation [9]

$$\Phi_0(r,\theta)=\frac{1}{4i}\int_a^b\mu\exp(-i\mu\pi)\sin\mu\pi\Psi(\theta,\mu)H_\mu^{(2)}(kr)\,d\mu \tag{9}$$

and from formula (4),

$$\Phi(r,\theta)=\frac{v_0}{4i\sqrt{r}}\int_{-i\infty}^{+i\infty}\mu\exp(-i\mu\pi)\sin\mu\pi H_\mu^{(2)}(kr)\frac{P_{\mu-1/2}(\cos\theta)}{\dfrac{dP_{\mu-1(2}(\cos\beta)}{d\beta}}\times$$

$$\times\int_a^b\sqrt{r_0}H_\mu^{(2)}(kr_0)\,dr_0\,d\mu. \tag{10}$$

In order to calculate the integral over the variable μ, formula (10), representing the acoustic potential, can be changed to another form. From the expression [8, 12]

$$H_\mu^{(2)}(kr_0)=\frac{\exp(i\mu\pi)J_\mu(kr_0)-J_{-\mu}(kr_0)}{i\sin\mu\pi}, \tag{11}$$

$$\Phi(r,\theta)=-\frac{v_0}{4\sqrt{r}}\int_{-i\infty}^{+i\infty}\mu H_\mu^{(2)}(kr)\frac{P_{\mu-1/2}(\cos\theta)}{\dfrac{dP_{\mu-1/2}(\cos\beta)}{d\beta}}\left(\int_a^b\sqrt{r_0}J_\mu(kr_0)\,dr_0\right)d\mu+$$

$$+\frac{v_0}{4\sqrt{r}}\int_{-i\infty}^{+i\infty}\mu\exp(-i\mu\pi)H_\mu^{(2)}\frac{P_{\mu-1/2}(\cos\theta)}{\dfrac{dP_{\mu-1/2}(\cos\beta)}{d\beta}}\left(\int_a^b\sqrt{r_0}J_{-\mu}(kr_0)\,dr_0\right)d\mu, \tag{12}$$

where J_μ is a Bessel function of the nth order. A new variable, $\mu = -\nu$, is introduced to the other of these integrals. From the relations for the Hankel function [12]

$$H_\nu^{(2)}(kr) = \exp(i\nu\pi) H_{-\nu}^{(2)}(kr) \tag{13}$$

and the Legendre function [7, 12]

$$P_{\nu-1/2}(\cos\theta) = P_{-\nu-1/2}(\cos\theta), \tag{14}$$

$$\int_{-i\infty}^{+i\infty} \mu \exp(-i\mu\pi) H_\mu^{(2)}(kr) \frac{P_{\mu-1/2}(\cos\theta)}{\dfrac{dP_{\mu-1/2}(\cos\beta)}{d\beta}} \left(\int_a^b \sqrt{r_0} J_{-\mu}(kr_0)\, dr_0 \right) d\mu$$

$$= -\int_{-i\infty}^{+i\infty} \nu H_\nu^{(2)}(kr) \frac{P_{\nu-1/2}(\cos\theta)}{\dfrac{dP_{\nu-1/2}(\cos\beta)}{d\beta}} \left(\int_a^b \sqrt{r_0} J_\nu(kr_0)\, dr_0 \right) d\nu. \tag{15}$$

The integral derived here has the same form as the first integral in formula (12). Hence the acoustic potential of the source situated on the cone becomes

$$\Phi(r, \theta) = -\frac{v_0}{2\sqrt{r}} \int_{-i\infty}^{+i\infty} \mu H_\mu^{(2)}(kr) \frac{P_{\mu-1/2}(\cos\theta)}{\dfrac{dP_{\mu-1/2}(\cos\beta)}{d\beta}} \left(\int_a^b \sqrt{r_0} J_\mu(kr_0)\, dr_0 \right) d\mu. \tag{16}$$

The integral from $-i\infty$ to $+i\infty$ can be calculated by using the method for calculating contour integrals. To this end, the integration contour is complemented with a semicircle with an infinitely long radius, situated to the right of the imaginary axis. The integral over the semicircle is zero for $r \geqslant b$. This can be shown by using the asymptotic representations for the Bessel [9] and Legendre functions [3, 7]. For high values of μ

$$J_\mu(kr) \int_a^b \sqrt{r_0} J_\mu(kr_0)\, dr_0 \sim \frac{1}{2\pi} \left(\frac{kr}{2}\right)^\mu \frac{\exp(2\mu)}{\mu^{2(\mu+1)}} \left[b^{3/2} \left(\frac{kb}{2}\right)^\mu - a^{3/2} \left(\frac{ka}{2}\right)^\mu \right], \tag{17}$$

$$J_{-\mu}(kr) \int_a^b \sqrt{r_0} J_\mu(kr_0)\, dr_0 \sim \frac{\sin\mu\pi}{\pi\mu^2} \left[b^{3/2} \left(\frac{b}{r}\right)^\mu - a^{3/2} \left(\frac{a}{r}\right)^\mu \right], \tag{18}$$

$$\frac{P_{\mu-1/2}(\cos\theta)}{\dfrac{dP_{\mu-1/2}(\cos\beta)}{d\beta}} \sim \frac{1}{\mu} \exp[\pm i\mu(\beta - \theta)], \tag{19}$$

where the sign (+) refers to this part of the right half-plane where $\mathrm{Im}(\mu) > 0$; the sign (−), to that with $\mathrm{Im}(\mu) < 0$.

The subintegral function occurring in formula (16) has its poles at points where

$$\frac{dP_{\mu-1/2}(\cos\beta)}{d\beta} = 0. \tag{20}$$

The poles are single and occur on the real axis [2, 3, 17]. Application of residua theory to the integral over a closed contour [10] gives the acoustic potential of the source situated on a cone, in the form of an infinite series,

$$\Phi(r,\theta) = \frac{iv_0\pi}{2\sqrt{r}} \sum_{n=1}^{\infty} (2\nu_n+1) H_{\nu_n+1/2}(kr) \left.\frac{P_{\nu_n}(\cos\theta)}{\dfrac{\partial^2 P_\nu(\cos\beta)}{\partial\nu\,\partial\beta}}\right|_{\nu=\nu_n} \times$$

$$\times \int_a^b \sqrt{r_0} J_{\nu_n+1/2}(kr_0)\,dr_0 \tag{21}$$

for $r \geqslant b$. In this formula summation is carried out over all the positive roots $\nu_n = \mu_n - 1/2$ of equation (20).

In order to obtain the potential for the region $a \geqslant r$, it is possible to use formula (10), in which the Hankel function $H_\mu^{(2)}(kr)$ can be represented by formula (11). Proceeding in an analogous way to the previous case, we obtain

$$\Phi(r,\theta) = -\frac{v_0}{2\sqrt{r}} \int_{-i\infty}^{+i\infty} \mu J_\mu(kr) \frac{P_{\mu-1/2}(\cos\theta)}{\dfrac{dP_{\mu-1/2}(\cos\beta)}{d\beta}} \left(\int_a^b \sqrt{r_0} H_\mu^{(2)}(kr_0)\,dr_0 \right) d\mu$$

$$= \frac{iv_0\pi}{2\sqrt{r}} \sum_{n=0}^{\infty} (2\nu_n+1) J_{\nu_n+1/2}(kr) \left.\frac{P_{\nu_n}(\cos\theta)}{\dfrac{\partial^2 P_\nu(\cos\beta)}{\partial\nu\,\partial\beta}}\right|_{\nu=\nu_n} \int_a^b \sqrt{r_0} H_{\nu_n+1/2}(kr_0)\,dr_0. \tag{22}$$

From formulae (21) and (22), the acoustic potential can be obtained for the region $a < r < b$,

$$\Phi(r,\theta) = \frac{iv_0\pi}{2\sqrt{r}} \sum_{n=0}^{\infty} (2\nu_n+1) \left.\frac{P_{\nu_a}(\cos\theta)}{\dfrac{\partial^2 P_\nu(\cos\beta)}{\partial\nu\,\partial\beta}}\right|_{\nu=\nu_n} \times$$

$$\times \left[H_{\nu_n+1/2}^{(2)}(kr) \int_a^r \sqrt{r_0} J_{\nu_n+1/2}(kr_0)\,dr_0 + J_{\nu_n+1/2}(kr) \int_r^b \sqrt{r_0} H_{\nu_n+1/2}^{(2)}(kr_0)\,dr_0 \right]. \tag{23}$$

In formulae (22) and (23) summation is also carried out over all the positive roots $\nu_n = \mu_n - 1/2$ of equation (20).

3. Acoustic field on the axis of a cone

There is the following relationship between the pressure and the acoustic potential Φ for harmonic vibrations [11, 17],

$$p = i\omega\varrho\Phi, \tag{24}$$

where ω — angular frequency, ϱ — density of the medium. In order to derive expressions for the acoustic pressure of a source situated on the cone, formulae (21)–(23) should be multiplied by $i\omega\varrho$.

One of the quantities characterizing the acoustic field is the distribution of the field on the main axis of the source. It is convenient to calculate the acoustic field of a source situated on the cone on the axis z. Assuming that $\theta = 0$ and considering that

$$P_{\nu_n}(1) = 1, \tag{25}$$

the following expressions are derived for the acoustic pressure on the axis of the cone,

$$p(z) = -\frac{\omega\varrho v_0\pi}{2\sqrt{z}} \sum_{n=0}^{\infty} \frac{2\nu_n+1}{\left.\dfrac{\partial^2 P_\nu(\cos\beta)}{\partial\nu\partial\beta}\right|_{\nu=\nu_n}} H^{(2)}_{\nu_n+1/2}(kz) \int_a^b \sqrt{r_0} J_{\nu_n+1/2}(kr_0)\, dr_0 \tag{26}$$

for $z \geqslant b$,

$$p(z) = -\frac{\omega\varrho v_0\pi}{2\sqrt{z}} \sum_{n=0}^{\infty} \frac{2\nu_n+1}{\left.\dfrac{\partial^2 P_\nu(\cos\beta)}{\partial\nu\partial\beta}\right|_{\nu=\nu_n}} \left[H^{(2)}_{\nu_n+1/2}(kz) \int_a^z \sqrt{r_0} J_{\nu_n+1/2}(kr_0)\, dr_0 + J_{\nu_n+1/2}(kz) \int_z^b \sqrt{r_0} H^{(2)}_{\nu_n+1/2}(kr_0)\, dr_0\right]. \tag{27}$$

for $a < z < b$,

$$p(z) = -\frac{\omega\varrho v_0\pi}{2\sqrt{z}} \sum_{n=0}^{\infty} \frac{2\nu_n+1}{\left.\dfrac{\partial^2 P(\cos\beta)}{\partial\nu\partial\beta}\right|_{\nu=\nu_n}} J_{\nu_n+1/2}(kz) \int_a^b \sqrt{r_0} H^{(2)}_{\nu_n+1/2}(kr_0)\, dr_0 \tag{28}$$

for $a \geqslant z$.

Assumption in the above formulae that $\beta = 90°$ permits the acoustic pressure on the axis of a circular ring situated in a planar, rigid baffle to be obtained. For $\beta = 90°$ the roots of equation (20) are [2, 7, 12]:

$$\nu_n = 2n, \quad n = 0, 1, 2, \ldots \tag{29}$$

and

$$\left.\frac{\partial^2 P(\cos\beta)}{\partial\nu\partial\beta}\right|_{\substack{\nu=2n \\ \beta=90°}} = (-1)^{n+1} \frac{2^{2n}(n!)^2}{(2n)!}. \tag{30}$$

Hence

$$p(z) = \frac{\omega\varrho v_0\pi}{2\sqrt{z}} \sum_{n=0}^{\infty} (-1)^n \frac{(4n+1)(2n)!}{2^{2n}(n!)^2} H^{(2)}_{2n+1/2}(kz) \int_a^b \sqrt{r_0} J_{2n+1/2}(kr_0) dr_0 \quad (31)$$

for $z \geqslant b$,

$$p(z) = \frac{\omega\varrho v_0\pi}{2\sqrt{z}} \sum_{n=0}^{\infty} (-1)^n \frac{(4n+1)(2n)!}{2^{2n}(n!)^2} \left[H^{(2)}_{2n+1/2}(kz) \int_a^z \sqrt{r_0} J_{2n+1/2}(kr_0) dr_0 + \right.$$

$$\left. + J_{2n+1/2}(kz) \int_z^b \sqrt{r_0} H^{(2)}_{2n+1/2}(kr_0) dr_0 \right] \quad (32)$$

for $a < z < b$,

$$p(z) = \frac{\omega\varrho v_0\pi}{2\sqrt{z}} \sum_{n=0}^{\infty} (-1)^n \frac{(4n+1)(2n)!}{2^{2n}(n!)^2} J_{2n+1/2}(kz) \int_a^b \sqrt{r_0} H^{(2)}_{2n+1/2}(kr_0) dr_0 \quad (33)$$

for $a \geqslant z$.

In order to calculate the sums of series occurring in formulae (31)–(33), it is possible to use an expansion of the function $\exp(-ikR)/R$ into a series of Legendre polynomials and cylindrical functions [12],

$$\frac{\exp(-ikR)}{R} = -\frac{i\pi}{2\sqrt{rr_0}} \sum_{n=0}^{\infty} (2n+1) J_{2n+1/2}(kr_0) H^{(2)}_{n+1/2}(kr) P_n(\cos\theta) \quad (34)$$

for $r > r_0$, where $R = \sqrt{r^2 + r_0^2 - 2rr_0\cos\theta}$. Assuming in the above formula that $\theta = \pi/2$ and taking into account the value of Legendre polynomials at this point [7, 12],

$$\frac{\exp(-ikR)}{R} = -\frac{i\pi}{2\sqrt{rr_0}} \sum_{n=0}^{\infty} (4n+1) \frac{(2n)!}{2^{2n}(n!)^2} J_{2n+1/2}(kr_0) H^{(2)}_{2n+1/2}(kr), \quad (35)$$

where $R = \sqrt{r^2 + r_0^2}$.

Considering formula (35), expressions (31)–(33) can be written in the form

$$p(z) = i\omega\varrho v_0 \int_a^b \frac{\exp(-ikR)}{R} r_0 dr_0. \quad (36)$$

After integration we obtain

$$p(z) = 2i\varrho c v_0 \sin\frac{k}{2}(r_b - r_a) \exp\left[-\frac{i}{2} k(r_b + r_a)\right], \quad (37)$$

where $\omega = kc$, $r_a = \sqrt{a^2 + z^2}$, $r_b = \sqrt{b^2 + z^2}$.

Expression (37) represents the acoustic pressure on the axis of a circular ring with radii a and b. Assumption that $a = 0$ gives a formula which defines

the pressure distribution on the axis of the circular piston situated in a planar, rigid baffle. An analogous formula was obtained in papers [11, 13, 17] by using other methods.

When the observation point is at a large distance from the top of the cone ($kz \gg 1$), for very low values of ka and kb ($ka < kb \ll 1$), from formula (26),

$$p(z) = \frac{i\varrho c v_0}{2} \cot\frac{\beta}{2}\left[(kb)^2 - (ka)^2\right]\frac{\exp(-ikz)}{kz}. \tag{38}$$

It follows therefrom that as the divergence angle of a cone, β, increases and as the distance of the observation point from the source increases, the pressure amplitude decreases. With the above assumptions formula (38) is valid for the whole variability interval of the angle θ. This source thus lacks directionality.

Assumption that $z = 0$ in formula (28) gives the expression

$$p(z) = 2i\varrho c v_0 \cot\frac{\beta}{2}\sin\frac{kb-ka}{2}\exp\left(-i\,\frac{ka+kb}{2}\right), \tag{39}$$

which represents the acoustic pressure on the top of the cone.

4. Conclusion

The expressions derived in the present paper for the acoustic potential and pressure are given in the form of infinite series. The series are divergent the faster, the greater the difference is between the observation point and

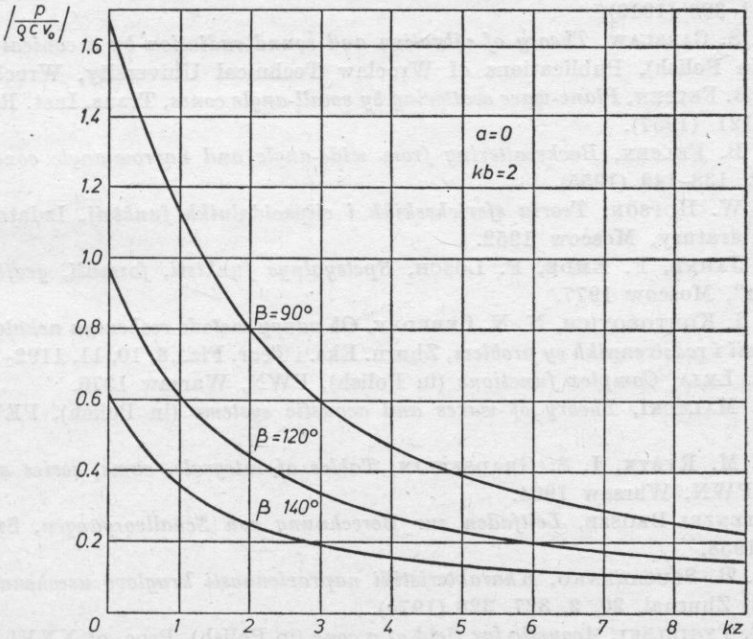

Fig. 2. The acoustic field on the axis of a circular cone. It is assumed that $a = 0$, $kb = 2$

the radial coordinates of the source (a, b). In a case when the cone divergence angle is 90°, the expression is obtained for the acoustic pressure on the axis of the circular ring, characterized by simple notation form.

On the basis of the results presented, numerical calculations were carried out of the absolute value of the relative pressure (the ratio of the absolute value of the pressure $|p|$ and the self resistance of the medium, ϱc, and the vibration velocity amplitude at the source, v_0) on the axis of the cone, depending on the parameter kz. It was assumed that $a = 0$, $kb = 2$, $\beta = 90°$, 120° and 140°. The tables of roots of equation (20), given in paper [2] were used in the calculations. The behaviour of relative pressure changes is shown in Fig. 2.

The expressions derived for the acoustic potential and pressure can be used for calculations of the acoustic far field and acoustic impedance. These problems will be considered in another paper.

References

[1] R. W. Carlise, *Conditions for wide angle radiation from conical sound radiators*, J. Acoust. Soc. Am., **15**, 1, 44–49 (1943).

[2] F. A. Carrus, C. G. Treuenfels, *Tables of roots and incomplete integrals of associated Legendre functions of fractional orders*, J. Math. and Phys., **29**, 4, 282–299 (1951).

[3] H. S. Carslaw, *Diffraction of waves by a wedge of any angle*, Proc. London Math. Soc., **19**, 291–306 (1919).

[4] H. S. Carslaw, *Theory of vibration and sound radiation by a conical loudspeaker membrane* (in Polish), Publications of Wrocław Technical University, Wrocław 1978.

[5] L. B. Felsen, *Plane-wave scattering by small-angle cones*, Trans. Inst. Radio Engrs., **AP–5**, 109–121 (1957).

[6] L. B. Felsen, *Backscattering from wide-angle and narrow-angle cones*, J. Appl. Phys., **26**, 2, 138–149 (1955).

[7] E. W. Hopson, *Teoria sfericheskikh i elipsoidalnikh funktsij*, Izdatelstvo Innostrannoy Literatury, Moscow 1952.

[8] E. Jahne, F. Emde, F. Lösch, *Spetsyalnye funktsii, formuli, grafiki, tablitsy*, Izd. "Nauka", Moscow 1977.

[9] M. I. Kontorovich, N. N. Lebedev, *Ob adnoy metode resheniya nekatorikh zadach teorii difraktsii i rodstvennikh ey problem*, Zhurn. Eks. i Teor. Fiz., **8**, 10, 11, 1192–1206 (1938).

[10] F. Leja, *Complex functions* (in Polish), PWN, Warsaw 1976.

[11] I. Malecki, *Theory of waves and acoustic systems* (in Polish), PEW, Warsaw 1964.

[12] I. M. Ryżyk, I. S. Gradsztejn, *Tables of integrals, sums, series and products* (in Polish), PWN, Warsaw 1964.

[13] Stenzel-Brosze, *Leitfaden zur Berechnung von Schallvorgängen*, Springer-Verlag, Berlin 1958.

[14] L. B. Slusarenko, *Kharakteristiki napravlennosti kruglovo usechennogo konusa*, Akusticheskij Zhurnal, **20**, 2, 327, 328 (1974).

[15] H. Tygielski, *Acoustic far field of a cone* (in Polish), Proc. of XXVI Open Seminar on Acoustics, Wrocław – Oleśnica, 1979, 508–511.

[16] Y. V. VAYSLEYB, *Rasseyanie zvukovikh voln na konechnom konuse*, Akusticheskij Zhurnal, **17**, 1, 33–42 (1971).

[17] R. WYRZYKOWSKI, *Linear theory of the acoustic field of gaseous media* (in Polish), Higher Pedagogical School, Rzeszów 1975.

[18] M. I. ZHURINA, W. M. KARMAZINA, *Tablitsy i formuli dla sfericheskikh funktsij* $P^m_{-1/2+i\tau}(x)$, **1**, **2** Izd. AN SSSR, Moscow 1960, 1962.

Received on 8 September, 1983.

ARCHIVES OF ACOUSTICS
9, 3, 317-326 (1984)

SOUND TRANSMISSION THROUGH SLITS AND CIRCULAR APERTURES

A. TROCHIDIS

Department of Physics and Mathematics, School of Engineering,
University of Thessaloniki, Greece

G. PAPANIKOLAOU

Department of Electrical Engineering, School of Engineering,
University of Thessaloniki, Greece

In this paper the sound transmission through slits and circular apertures is examined. Approximate theoretical expressions for the transmission loss are derived using simple energy balance considerations. Both resonant and nonresonant transmissions are taken into account. Theoretical values of the transmission loss are compared with measurements.

1. Introduction

The transmission of sound through small apertures (circular or narrow slit-shaped) is of interest in many noise control problems and in particular in architectural acoustics. Slits and apertures are found in most typical partitions decreasing their sound insulation.

Theories for the transmission of sound through slits and circular apertures have been advanced by several authors [1, 2, 3, 4]. All these theories in spite of their exact mathematical formulation are rather complicated to be used in cases of practical interest.

The aim of this paper is to show that using simple energy balance equations well known from *S.E.A.* (statistical energy analysis) approximate expressions for the transmission loss of small apertures can be obtained. Comparison between measurements and theoretical predictions by means of the obtained formulae is found to be in good agreement for all partical cases.

2. Theoretical transmission loss

We consider the transmission suite shown in Fig. 1. The coupling element between the two rooms is a small aperture (slit or circular opening). The whole system may be considered to consist of three coupled subsystems as shown schematically in Fig. 2. Subsystems 1, 2 and 3 represent source room, aperture and receiving room respectively.

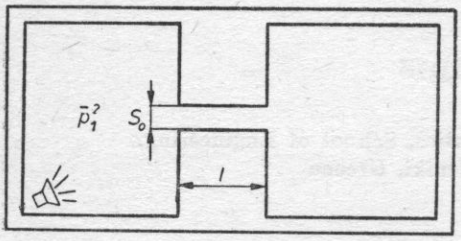

Fig. 1. Transmission suite

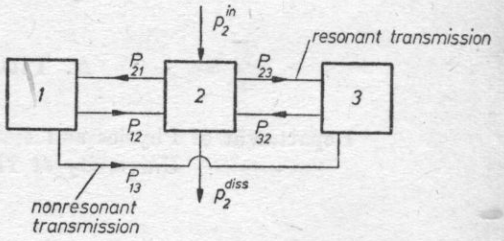

Fig. 2. Block diagram of power flow between the three coupled systems

In case of acoustical excitation of the source room, the power transmitted to the receiving room is made up of the contribution of nonresonant and resonant transmission. The nonresonant transmission, represented by the power flow P_{13} directly from system 1 to 3, is due to modes that are resonant outside of the frequency band under consideration. In this situation, system 2 acts only as a coupling element for the sound transmission between systems 1 and 3. This forced power flow is responsible for the "mass law" transmission at low frequencies. The resonant transmission, represented by the power flow P_{12}, i.e. P_{23}, is due to resonant modes and is dominant in higher frequencies as the wavelength of sound becomes comparable to the depth of the aperture.

a) Nonresonant transmission

Referring to Fig. 1 and considering that the dimensions of the opening are small compared to the wavelength, there will be a sound pressure doubling at the face S_0 of the opening due to sound reflection. If $Z_0 = R_0 + j\omega M_0$ is the acoustic impedance of the opening and M the radiation mass loading due to its finite depth, the sound power transmitted through the opening can be expressed as

$$P_{\mathrm{tr}} = \frac{4\bar{p}^2 S_0^2}{|2Z_0 + j\omega M|^2} R_0, \tag{1}$$

where $\bar{p}^2$ is the mean square pressure in the source room. For low frequencies the radiation resistance R_0 in the denominator can be neglected so that equa-

tion (1) simplifies into:

$$P_{\mathrm{tr}} = \frac{4\overline{p}^2 S_0^2}{\omega^2(2M_0+M)^2} R_0. \tag{2}$$

In case of a circular aperture of a radius a the radiation resistance at low frequencies is [5]:

$$R_a = \varrho c \frac{a^2 k^2 S_a}{2}, \tag{3}$$

where $k = \omega/c$ the corresponding wave number.

The total effective mass $2M+M$ can be expressed as [6]:

$$2M_0+M = \frac{\varrho S_a^2}{G_a}, \tag{4}$$

where $G_a = \dfrac{S_a}{l_{\mathrm{eff}}}$, with $l_{\mathrm{eff}} = l+1,7a$ [5], is the effective length of the opening.

Using equations (3) and (4), the transmitted sound power can be written as:

$$P_{\mathrm{tr}} = \frac{2\overline{p}^2 S_a}{\varrho c}\left(\frac{a}{l_{\mathrm{eff}}}\right)^2. \tag{5}$$

Thus, the nonresonant transmission loss of a circular aperture, referring to the total wall area, will be:

$$10\log\frac{P_{\mathrm{in}}}{P_{\mathrm{tr}}} = 10\log\frac{\left(\dfrac{\overline{p}^2 S_w}{\varrho c}\right)}{\left(\dfrac{2\overline{p}^2 S_a}{\varrho c}\right)}\left(\frac{l_{\mathrm{eff}}}{a}\right)^2 = 10\log\frac{1}{2}\left(\frac{S_w}{S_a}\right)+20\log\left(\frac{l_{\mathrm{eff}}}{a}\right), \tag{6}$$

where $P_{\mathrm{in}} = \dfrac{\overline{p}^2 S_w}{\varrho c}$ the incident sound power on the wall area S_w.

In case of a long narrow slit the sound power transmitted can be similarly expressed as:

$$P_{\mathrm{tr}} = \frac{4\overline{p}^2 S_s^2}{|2Z_s+j\omega M|^2} R_s, \tag{7}$$

where R_s is the radiation resistance, Z_s the impedance and S_s the surface of the slit.

The radiation resistance of a long narrow slit at low frequencies is [6]:

$$R_s = \frac{\varrho c k S_s}{4}, \tag{8}$$

where b is the breadth of the slit and S_s its cross section.

The effective mass can be expressed as [6]:

$$2M_s + M = \frac{\varrho S_s^2}{G_s} \tag{9}$$

with $1/G_s = (1/b) + 0.7 + \frac{2}{\pi} 1\eta\left(\frac{2c}{\omega b}\right)$ per unit length, where l is the depth and b the breadth of the slit. Substituting the values of R_s and effective mass in equation (7) we obtain for the transmitted power

$$P_{\text{tr}} = \frac{\overline{p}^2 L}{\omega \varrho} \frac{1}{\left[l/b + 0.7 + \frac{2}{\pi} \ln \frac{2c}{\omega b}\right]^2}, \tag{10}$$

where L is the length of the slit. The corresponding nonresonant transmission loss of the slit can be written in the form:

$$TL_s = \frac{P_{\text{in}}}{P_{\text{tr}}} = 10\log \frac{\omega S_w}{cL} G_s^2 = 10\log \frac{\omega S_w}{cL} + 20\log[(l/b) + 0.7 + \frac{2}{\pi} \ln \frac{c^2}{\omega b}. \tag{11}$$

b. Resonant transmission

At higher frequencies, as the wavelength becomes comparable to the depth of the opening ($\lambda \sim l$), system 2 becomes resonant and modes are excited and the sound power is transmitted to the receiving room.

In this case, the power balance equation expressing the principle of energy conservation for the opening as a system (neglecting the power flow from the receiving room back to the source room) can be written as

$$p_2^{\text{in}} = p_2^d + P_{23} + P_{21}, \tag{12}$$

where p_2^{in} denotes the power supplied to the opening, p_2^d the power dissipation in the opening and P_{23}, P_{21}' the power flow from the opening (system 2) to the rooms (systems 1 and 3).

The dissipation of stored energy in system 2 can be expressed as:

$$p_2^d = \omega n_2 E_2, \tag{13}$$

where n_2 is the loss factor of the opening and E_2 the stored energy. The power flow P_{23}, P_{21} to the rooms following *S.E.A.* [7] can be respectively expressed as:

$$P_{23} = P_{21} = \omega n_{23} E_2, \tag{14}$$

where n_{23} is the parameter called coupling loss factor, representing the losses of system 2 due to its coupling to the rooms. The input power supplied to the opening is:

$$p_{\text{in}}^2 = \omega n_{12} E_1, \tag{15}$$

with n_{12} the coupling loss factor between source room and opening and E_1 the energy stored in source room.

Substituting equations (13), (14) and (15) in (12) we obtain the following equation:

$$\omega n_{12} E_1 = \omega n_2 E_2 + 2\omega n_{21} E_2. \tag{16}$$

The energy stored in the source room can be written as

$$E_1 = \frac{V_1 \overline{p}_1^2}{\varrho c^2}, \tag{17}$$

where $\overline{p}_1^2$ is the mean square pressure and V_1 the volume of the source room, while the energy stored in the opening

$$E_2 = m_2 \overline{v}_2^2, \tag{18}$$

where m_2 – the air mass and $\overline{v}_2^2$ – the mean square velocity of the opening. Combining equations (16), (17) and (18) as follows:

$$n_{12} \frac{V_1}{\varrho c^2} \overline{p}_1^2 = n_2 m_2 \overline{v}_2^2 + 2 n_{21} m_2 \overline{v}_2^2 \tag{19}$$

and solving for the mean square velocity of the opening we obtain:

$$\overline{v}_2^2 = \overline{p}_1^2 \frac{V_1}{V_2} \frac{1}{\varrho^2 c^2} \frac{n_{12}}{n_{21}} \frac{1}{2 + \dfrac{n_2}{n_{21}}}. \tag{20}$$

The power radiated from the opening to the receiving room P_{23}, i.e. P_{21}, can be expressed as:

$$P_{23} = P_{21} = \omega n_{21} m_2 \overline{v}_2^2 = \varrho c S_2 \sigma_2 \overline{v}_2^2, \tag{21}$$

where σ_2 is the radiation efficiency of the opening.

It follows for the coupling loss factor n_{21}:

$$n_{21} = \frac{\sigma_2}{kl}. \tag{22}$$

Furthermore, from the statistical energy analysis it is well known [7] that the ratio of the coupling loss factor in two opposite directions is inversely proportional to the corresponding model densities, i.e.

$$\frac{n_{12}}{n_{21}} = \frac{N_2}{N_1}, \tag{23}$$

where N_1, N_2 are the model densities of the source room and the opening respectively.

Using equations (22) and (23) we obtain for the mean square velocity of the opening:

$$\overline{v}_2^2 = \overline{p}_1^2 \frac{V_1}{V_2} \frac{1}{\varrho^2 c^2} \frac{N_2}{N_1} \frac{1}{2\left(1+\dfrac{n_2 kl}{\sigma_2}\right)}, \tag{24}$$

and for the power transmitted through the opening:

$$P_{\mathrm{tr}} = \varrho c S_2 \sigma_2 \overline{v}_2^2 = \overline{p}_1^2 \frac{V_1}{2} S_2 \frac{\sigma_2}{\varrho c} \frac{N_2}{N_1} \frac{1}{2\left(1+\dfrac{n_2 kl}{\sigma_2}\right)}. \tag{25}$$

In case of a circular aperture [8]

$$N_2 = \frac{1}{c\pi}, \qquad N_1 = \frac{V_1 \omega^2}{2\pi^2 c^3}. \tag{26}$$

So that (25) can be written in the form:

$$P_{\mathrm{tr}} = \overline{p}_1^2 \frac{c}{\varrho c} \sigma_a \frac{1}{\left(1+\dfrac{n_2 kl}{\sigma_a}\right)}. \tag{27}$$

In case of a long narrow slit [8]:

$$N_2 = \frac{l S_s \omega}{4\pi c^2 b}, \tag{28}$$

so that from equation (25) it can be obtained for the transmitted power:

$$P_{\mathrm{tr}} = \overline{p}_1^2 \frac{S_s \sigma_s}{4\varrho b \omega} \frac{\pi}{\left(1+\dfrac{n_2 kl}{\sigma_s}\right)}. \tag{29}$$

WILSON and SOROKA [9] have shown that the change from a circular piston to a square one produces only a slight change in radiation resistance and hence, it is quite appropriate to apply impedance functions for circular pistons to the case of a square piston by substituting the value of the radius a with the equivalent "radius" $(S_s/\pi)^{1/2}$. Exact expressions for the radiation resistance of a circular or an equivalent rectangular piston have been given earlier [9, 10] in the form:

$$R\left[2k\left(\frac{S}{\pi}\right)^{1/2}\right] = \frac{2}{\pi} \sum_{n=0}^{\infty} \frac{B_{2n}\left[k\left(\dfrac{S}{\pi}\right)^{1/2}\right]^{2n+2}}{(2n+3)!} \pi^{n+1}, \tag{30}$$

where B_{2n} are coefficients depending on the geometry of the opening.

Using the values of the radiation resistance given by equation (30) the resonant power transmission can be obtained.

c. Overall transmission

The sound power transmitted to the receiving room through the opening is made up of the contribution of nonresonant and resonant transmission. Combining equations (5), (10), (27) and (29) a composite transmission loss for all frequencies can be obtained.

In case of a circular aperture we easily obtain:

$$TL = 10\log\left\{\frac{1}{4}\left(\frac{S_w}{S_a}\right)\frac{1}{\left[2\left(\frac{a}{l_{\text{eff}}}\right)^2+\frac{c^2\sigma_a}{S_a\omega^2}\right]}\right\} \tag{31}$$

and in case of a narrow slit respectively:

$$TL = 10\log\left\{\left(\frac{S_w}{S_s}\right)\frac{1}{\left[\frac{4cL}{\omega S_s}\frac{1}{\left[1/b+0.7+\frac{2}{\pi}\ln\frac{2c}{\omega b}\right]^2}+\frac{\pi c\sigma_s}{\omega b}\right]}\right\}. \tag{32}$$

In both cases we have assumed undamped conditions, so that the energy dissipation can be neglected.

At low frequencies the first term in the denominator dominates, so that the transmission loss follows practically the "mass law" transmission of equation (6) or (11). At higher frequencies the second term becomes predominant determining the sound transmission.

3. Comparison with experiment

The measurements were made between two small rooms. The aperture was made in the middle of a thick gypsum partition wall, while the microphone was mounted in the measuring room as near as possible to the orifice of the aperture.

Fig. 3 shows a comparison between the measured transmission loss of circular apertures of various cross section and that calculated using equation (31). The depth of the aperture, i.e. the thickness of the separation wall between the two rooms, was 5 cm.

Fig. 4 shows a similar comparison between experimental results and theoretical predictions using equation (32) for slits of various breadth. The depth of the slits, i.e. the thickness of the separation wall, was 7 cm and its length 60 cm.

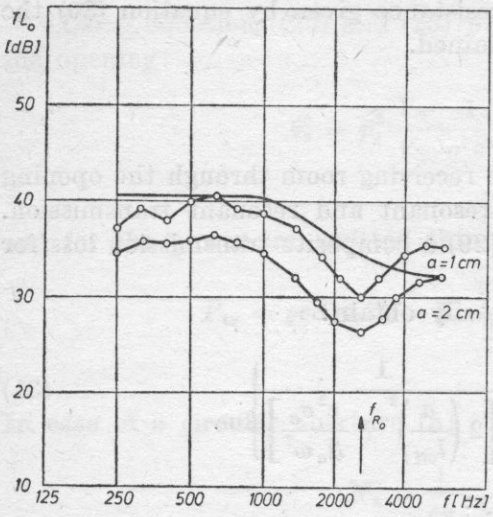

Fig. 3. Transmission loss of a 5 cm gypsum wall with a circular aperture of radius a in the middle

0 —— 0 experiment; ——— from equation (31)

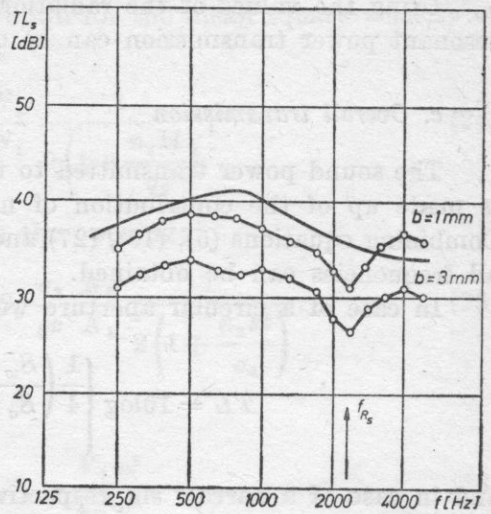

Fig. 4. Transmission loss of a 7 cm gypsum wall with a slit of length 0.60 m and variable breadth b

0 —— 0 experiment; ——— from equation (32

4. Discussion of results

The measured and theoretical transmission loss values for slits and circular apertures appear to be in good agreement at low frequencies. In this frequency range the sound transmission is not resonant following equations (6) and (11). Within the resonance domain, where the aperture resonates as a tube open at both ends at the frequency $f_R = \frac{c}{2L}$, the agreement between measurements and theoretical predictions is not so good, even though the main trends are predicted.

It seems that due to the statistical nature of our derivation we get a mean value of the transmission loss for the higher frequencies, which can be considered as satisfactory for practical use.

References

[1] C. J. Bouwkamp, *On the transmission of a circular aperture*, Physic. Rev., **75**, 608 (1949).

[2] Y. Nomura, S. Inavashiro, *On the transmission of acoustic waves through a circular channel of a thick wall*, Sci. Rep. Tohaku Univ., (1), 12 B, 57 (1960).

[3] M. C. Comperts, *The sound insulation of circular and slitshaped apertures*, Acustica, **14**, 1–16 (1964).

[4] A. SAUTER, W. SOROKA, *Sound transmission through rectangular slots of finite depth between reverberant rooms*, J. Acoust. Soc. Am., **47**, 5, 11 (1970).

[5] E. KINSLER, A. FREY, *Fundamentals of acoustics*, J. Wiley, New York, 1980, s. 226.

[6] E. SKUDRZYK, *Die Grundlagen der Akustik*, Springer, Wien, 1954, s. 349, 350.

[7] R. H. LYON, G. MAIDANIK, *Power flow between linearly coupled oscillators*, J. Acoust. Soc. Am., **34**, 623, 1962.

[8] L. CREMER, M. HECK, *Körperschall*, Springer, Berlin, 1973, s. 425.

[9] G. W. SWENSON, W. JOHNSON, *Radiation impedance of a rigid square piston in an infinite baffle*, J. Acoust. Soc. Am., **24** (1952).

[10] G. WILSON, W. SOROKA, *Approximation to the diffraction of sound by a circular aperture in a rigid wall of finite thickness*, J. Acoust. Soc. Am., **37**, 286 (1965).

Received on 4 September, 1983.

ARCHIVES OF ACOUSTICS
9, 3, 327-348 (1984)

DISTRIBUTION OF SOUND INTENSITY LEVEL OF FREQUENCY RESPONSES OF A ROOM

EDWARD OZIMEK

Institute of Acoustics, Adam Mickiewicz University
(60–759 Poznań, ul. Matejki 48/49)

In a number of investigations on the quantitative evaluation of the behaviour of the frequency response of a room, it has been assumed that above some boundary frequency this behaviour can be regarded as the result of a random process of summing up of reflected waves with an intensity level distribution close to a normal one. In the literature there is however lack of papers which confirm experimentally the correctness of this assumption or indicate its possible deviations from practical conditions. In view of this, investigations were undertaken to determine the form of the function of distribution of sound intensity level changes for a number of frequency responses registered in a few selected rooms (models) with varying acoustic properties. The investigation results obtained show that the functions of distribution of intensity level changes for these responses do sometimes differ a great deal from the normal one. This testifies that over the range of model investigations for which all the required conditions are satisfied, the assumption of a normal (Gaussian) distribution of the energy of reflected waves is not fulfilled.

1. Introduction

The purpose of the first papers [14, 1] on analysis of the behaviour of the frequency response of a room was mainly to determine for it such parameters as would describe quantitatively the irregularity of its behaviour. In these papers the frequency irregularity F of this response and the mean distance of its intensity level maxima were recognized to be the most essential parameters. A particularly detailed analysis of the behaviour of the frequency response was carried out in papers [9, 12], where new parameters were proposed for describing the behaviour of its irregularity and, as a result of theoretical considerations, some relationships between the mean distance of maxima of this response and the reverberation time of the room were derived. The properties of the frequency response were also considered from the point of view of correlation analysis [10]. The behaviour of the so-called frequency correla-

tion functions obtained in this range for these responses permitted the determination, with given reverberation conditions in the room, of the frequency range beyond which values of the frequency response are not correlated with each other. Interesting results of investigations on the behaviour of the frequency response were given by the most recent papers on the subject [6, 5, 3], in which a functional relationship was shown to exist between the standard deviation, determined for this response, and the value of the critical distance of the room. As a result, it was possible to develop a new method for determining this distance.

It is interesting to note that in a number of the papers mentioned above it is assumed a priori that over some boundary frequency, the behaviour of the frequency response of the room can be regarded as the result of a random process of summing up of reflected waves with an intensity level distribution close to a normal one. This approach to the frequency response permitted the authors of these papers to carry out an analytical description of its definite parameters using statistical methods [9, 11]. It should be noted, however, that in the literature there is lack of papers confirming experimentally the correctness of this assumption or indicating its possible deviations from practical conditions. The strictness of this assumption thus requires experimental verification, the more so when it is considered that the room itself is a complex physical system whose character is to a varying degree determinate and in which the random nature of phenomena, in strictly probabilistic terms, requires deeper justification and analysis. This point of view warrants a supposition that probability distribution functions characterizing the random nature of these phenomena, will depend in a specific manner on some physical and geometrical quantities, such as: the reverberation time of the room, the distance between the source and the receiver, the directionality of the source etc. Keeping this in mind, research was undertaken with the essential aim of determining the form of sound intensity level distribution functions for a number of frequency responses recorded in some chosen rooms and defining some of its statistical parameters for these functions.

2. Irregularity of the behaviour of the frequency response of the room

The frequency response of a room is expressed in general by the irregularity of the transmission by the room of the intensity of a sinusoidal signal with its frequency changing with given rate. This irregularity is most often represented by the parameter F [1], which defines the difference between the extreme sums (i.e. the maximum sums $L_{\max}$ and the minimum ones $L_{\min}$) of sound intensity levels of this response, measured in the consecutive frequency bands Δf:

$$F = \frac{\sum L_{\max} - \sum L_{\min}}{\Delta f}. \tag{1}$$

It should be noted that the value of the parameter F, defined by formula (1), depends only on the resultant (summary) dynamics of extrema which fall in the range Δf and does not take into account their number, which often causes some ambiguities. For example, when considering two behaviours of the frequency response which differ considerably from each other, with one characterized by a small number of maxima but their high dynamics, the other in turn having a large number of maxima but their low dynamics, it is possible to obtain for these behaviours in some cases similar values of F.

The results of investigations carried out by SCHROEDER [9, 11, 12] indicate that there exists a relationship between the parameter F of the frequency response and the reverberation time T of a room. This relationship, as expressed by formula (2), is valid for frequencies f lying over some boundary frequency f_b, defined by expression (3),

$$F_s \simeq 1.4\,\mathrm{T}, \tag{2}$$

where F_s – irregularity of the frequency response (acc. to SCHROEDER),

$$f \geqslant f_b = 4000\sqrt{T/V}, \tag{3}$$

where V – the volume of the room.

It follows from formula (2) that irregularity of the frequency response of a room is proportional to its reverberation time. Apart from studies of the irregularity of the frequency response of a room, research work was also carried out on the irregularity of the distribution of its maxima on the frequency scale. In their experimental papers, KUTTRUFF and THIELE [7] showed that the average spacing δf between adjacent maxima of the frequency response was inversely proportional to the reverberation time of the room.

$$\delta f \simeq \frac{6.7}{T}. \tag{4}$$

However, according to the later theoretical and experimental research [12], the average spacing between adjacent maxima of this response is less than that given by formula (4), being

$$\delta f \simeq \frac{3.9}{T}. \tag{5}$$

It should be added that the experimentally determined value of δf depends to a large extent on the parameters of the measuring system. E.g. according to paper [12], in determining the quantity δf sometimes results are obtained, which differ from each other by as much as about 50%, depending on the quantization properties of the recorder used for registering the frequency response.

The behaviour of the frequency response of a room is usually considered, for frequencies above some boundary value, as a result of statistical phenomena, based on the assumption of a random character of summing up of a direct wave and a large number of reflected waves, with different amplitudes and phases. This signifies that in describing the irregularity of the behaviour of this response, also other, more strictly defined mathematically than the quantity F, statistical parameters can be introduced, such as the mean square fluctuation of the frequency response and probability moments of higher order. Statistical treatment of this response as some random process with distribution close to a normal one provided the basis for investigations of its so-called frequency correlation function [10], according to which an analytical expression of this function has the form

$$\varrho(\delta f') = \frac{1}{4-\pi}\left[2(1+z)f\left(\frac{2\sqrt{z}}{1+z}\right)-\pi\right], \tag{6}$$

where $\delta f'$ — frequency interval (analogous to the time interval δt of the autocorrelation function $\varrho(\delta t)$), $z = [1+(2\pi\tau\delta f')]^{-1/2}$, $\tau = T/13.8$, $f(\ldots)$ — hypergeometrical function.

Analysis of the behaviour of the frequency autocorrelation function indicates that it shows a distinct tendency to decrease with increasing $\delta f'$, reaching a value of the order of 0.1 for the frequency interval $\delta f' = 6.6/T$. On this basis, it can be assumed that at frequency intervals, of $6/T$ approximately [Hz], values of the maxima of the frequency response of a room are independent of each other.

The assumption of a random sound pressure amplitude distribution in the room encouraged us to seek an analytical form of the probability density function of this distribution.

According to papers [12, 4], when a room is excited by signals with frequencies above some boundary value f_b, the probability density function of the sound pressure amplitude distribution at some distance from the source has the form

$$Pr(p) = \frac{2p}{\langle p_r^2\rangle}\exp\left(-\frac{p^2+p_d^2}{\langle p_r^2\rangle}\right)J_0\left(\frac{2pp_d}{\langle p_r^2\rangle}\right), \tag{7}$$

where p — the resultant sound pressure, composed of the sound pressure of the direct wave p_d, which is a deterministic component, and the sound pressure of the reflected waves $\langle p_r\rangle$, which is a random component; J_0 — a Bessel function of the first kind of the zeroth order; $\langle\rangle$ — averaging over the set of reflected waves.

Using the dependence $I \sim p^2$, the density function of the sound pressure amplitude distribution, $Pr(p)$, can be expressed as a function of the density

distribution of its intensity $Pr(I)$,

$$Pr(I) = \frac{1}{\langle I_r \rangle} \exp\left(-\frac{I+I_d}{\langle I_r \rangle}\right) J_0\left(\frac{2\sqrt{II_d}}{\langle I_r \rangle}\right), \tag{8}$$

where $I = I_d + I_r$ – the resultant sound intensity at a given measurement point.

Designating as D the ratio of the direct sound intensity I_d to the reflected (reverberant) sound intensity I_r, i.e.

$$D = \frac{I_d}{\langle I_r \rangle}, \tag{9}$$

and replacing intensity by its logarithmic measure, i.e. the intensity level L,

$$L = 10\log\frac{I}{\langle I \rangle} \quad [\text{dB}], \tag{10}$$

we obtain the expression of the probability density function of the sound intensity level distribution, depending on the parameter D, in the form

$$Pr(L) = k(1+D)\exp\{-[(1+D)\exp(kL)+D]+kL\} J_0\left\{2\sqrt{[(1+D)D\exp(kL)]}\right\}, \tag{11}$$

where $k = \ln 10/10 = 0.23$.

On the assumption that $D \to 0$, i.e. with $I_d \to 0$ (at a large distance from the source), the density function represented by expression (11) becomes (12):

$$Pr(L) = k\exp\left(kL - \exp(kL)\right) = 0.23\exp\left(0.23L - \exp(0.23L)\right). \tag{12}$$

It is interesting to add that for a definite distance in a source-microphone system the behaviour of frequency responses, recorded for changing the position of the system in a room, will be different from each other, sometimes quite considerably so; however, the statistical properties of these responses will be independent of this position (under the condition that the source-microphone system is not situated close to the surfaces enclosing the room). In turn, a change in the distance between the source and the microphone causes a change both in the behaviour of the frequency response and the value of the parameter D. This fact does not undermine, however, the validity of expression (11), which still describes the form of the probability density function of the distribution of these responses.

Knowledge of the probability density function of the intensity level, $Pr(L)$, of the frequency response of a room can permit the moments M of appropriate orders to be determined for it, according to formula (13),

$$\langle L^M \rangle = \int_{\infty}^{\infty} L^M Pr(L)\, dL. \tag{13}$$

For $M = 1$ the mean value of this function can be obtained,

$$\langle L \rangle = \int_{-\infty}^{\infty} LPr(L)dL, \tag{14}$$

whereas for $M = 2$ the mean square value

$$\langle L^2 \rangle = \int_{-\infty}^{\infty} L^2 Pr(L)dL. \tag{15}$$

can be determined.

From this, the value of the standard deviation σ of the function $Pr(L)$ can be found, from formula (16),

$$\sigma(D) = \sqrt{\langle L^2 \rangle - \langle L \rangle^2} = \sqrt{\int_{-\infty}^{\infty} L^2 Pr(L)dL - \left[\int_{-\infty}^{\infty} LPr(L)dL\right]^2}. \tag{16}$$

Fig. 1. shows a curve of the dependence of the standard deviation σ on the logarithmic value of the ratio of the direct sound intensity to the reverberant sound intensity [5]. It is seen in this picture that the measurement of the standard deviation of the frequency response permits the critical dis-

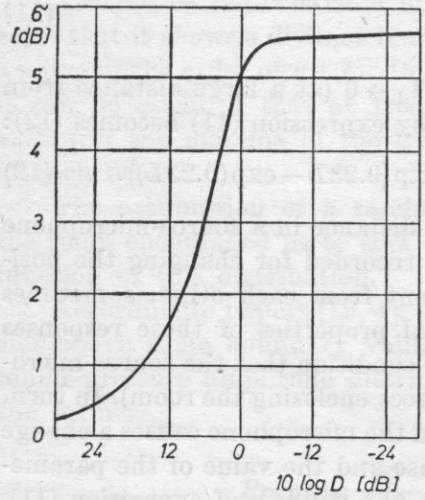

Fig. 1. The dependence of the standard deviation σ of the frequency response of a room on the value $10 \log D = 10 \log I_d/I_r$ [s]

tance of the room to be determined, i.e. the distance at which the quantity $D = I_d/\langle I_r \rangle$ is 1. This problem was considered in greater detail in papers [6, 5, 3]. It is also seen in this figure that in the reverberant field the standard deviation of the frequency response has a constant value of about 5.6 dB. It should be noted that the method proposed above for determining the critical distance from the measurement of the standard deviation of the frequency response assumes lack of directionality of the source and receiver. In practice, however,

these transducers always involve some directional effect, and accordingly, in determining exact values of this distance, the value of their directionality coefficients should be taken into account.

It can be seen from the above considerations that the behaviour of the frequency response of a room is usually regarded as a result of random processes of a type for which the form of the probability density function is assumed to be close to the density function of a normal distribution. This assumption had not been verified experimentally in previous investigations, neither for actual rooms, nor in model studies. Moreover, the possible deviations of the form of this function for practical distributions from those assumed in theoretical considerations are also unknown. This fact encouraged us to undertake investigations with the main aim of experimental verification of this assumption. This verification was carried out on the basis of analysis of the form of histograms of sound intensity level distribution, as determined for a number of frequency responses recorded in a few acoustically different model rooms which satisfied the condition $l \gg \lambda$. In addition, within the framework of the present investigations, the values of basic statistical parameters were also determined for these histograms.

3. Measurement object, investigation apparatus and method

The investigations were carried out in a special (model) room, in which four forms of interior with different acoustical properties could be shaped, designated below as rooms: B (damped), C (undamped), and D and E, which were acoustically coupled rooms, with different values of the coupling coefficient Q [8]. In rooms B and C measurement points were chosen; their situation is shown in Fig. 2. In addition this figure also shows the distribution

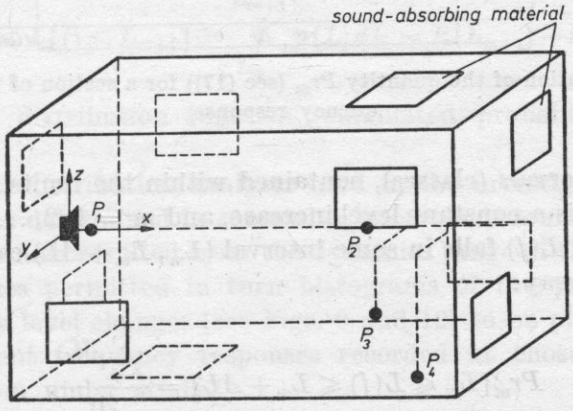

Fig. 2. The position of the measurement points $P_1 (x = 5, y = 0, z = 0)$, P_2 $(x = 100, y = 0, z = 0)$, P_3 $(x = 112, y = 20, z = 32)$, P_4 $(x = 135, y = 30, z = 60)$ and the distribution of absorbing materials in room B

of the absorbing material, with a mean absorption coefficient $a \simeq 0.6$ over the frequency range 630–4000 Hz, with which room B was damped.

A schematic diagram of the measurement apparatus system, in which an essential role was played by a statistical distribution analyser, connected to a unit of digital signal processing, is shown in Fig. 3.

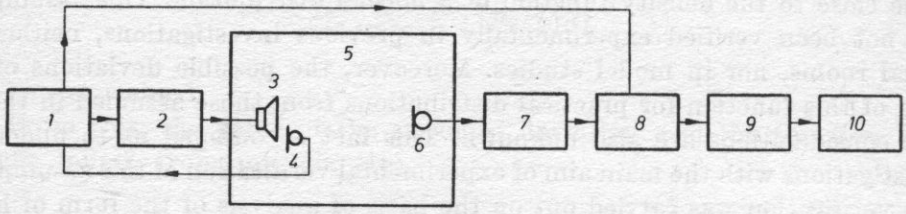

Fig. 3. A schematic diagram of the apparatus used for measuring the frequency response of a room

1 – generator, *2* – power amplifier, *3* – loudspeaker type 400 G, diameter 2 cm, *4* – compensation microphone (nondirectional, *B*–K), *5* – room investigated, *6* – measurement microphone nondirectional, B–K), *7* – microphone amplifier, *8* – plotter voltmeter, *9* – statistical distribution analyser, *10* – computer

Fig. 4 illustrates the essence of analysis of the behaviour of the frequency response. The intensity level $L(f)$, variable as a function of frequency, is divided

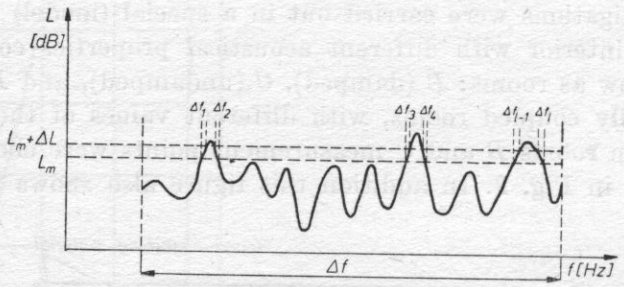

Fig. 4. An interpretation of the quantity Pr_m (see (17)) for a section of the curve of the frequency response

into adequate intervals (classes), contained within the limits from L_m to $L_m + \Delta L$, where ΔL is a constant level increase, and $m = 1, 2, \ldots, r$. The probability that the level $L(f)$ falls in some interval $(L_m, L_m + \Delta L)$ can be represented in the following way:

$$Pr_m[L_m \leqslant L(f) \leqslant L_m + \Delta L] = \frac{\sum_{i=1}^{l} \Delta f_i}{\Delta f}. \tag{17}$$

This magnitude of the probability Pr_m for successive intervals of the intensity level can be determined from indications of the statistical distribution

analyser. The values of Pr_m falling in particular intervals can be represented graphically by a histogram (see Fig. 5), which illustrates the probability distribution of sound intensity level changes over a given bandwidth Δf of the frequency response. Passing within the limits from ΔL to zero, we can obtain the

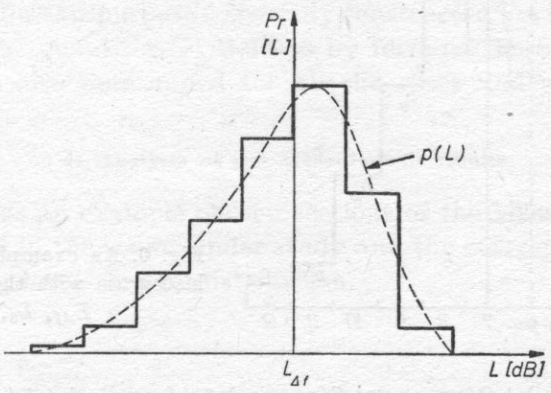

Fig. 5. An example of the histogram of the probability distribution of sound intensity level changes for the frequency response of a room

form of the probability density function $p(L)$, marked by dashed line in Fig. 5,

$$p(L) = \lim_{\Delta L \to 0} \frac{Pr_m[L_m \leqslant L(f) \leqslant L_m + \Delta L}{\Delta L}. \tag{18}$$

With this boundary condition, the probability that the function $L(f)$ takes a value from any interval (L_m, L_{m+1}) can be expressed by an integral of the probability density function within the limits of this interval, i.e.

$$Pr[L_m \leqslant L(f) \leqslant L_{m+1}] = \int_{L_m}^{L_{m+1}} p(L)\,dL = P(L_{m+1}) - P(L_m), \tag{19}$$

where $P(L)$ is a distribution function (cumulated probability distribution function).

The statistical distribution analyser used in the investigations permitted values of Pr_m to be determined in successive intervals of sound intensity level, each 5 dB wide (which resulted from the dynamics range of the potentiometer used). These values permitted in turn histograms of the probability distribution of intensity level changes (see Figs. 9 and 12) to be plotted for a large number of different frequency responses recorded at chosen measurement points of the room under study.

In addition, from indications of the statistical distribution analyser, the mean values of the intensity level $L_{\Delta f}$ and the standard deviation $\sigma_{\Delta f}$ from $L_{\Delta f}$ were also calculated from formulae (20) and (21) [2].

The symbols used in these formulae are defined, as an example, in the histogram given in Fig. 6.

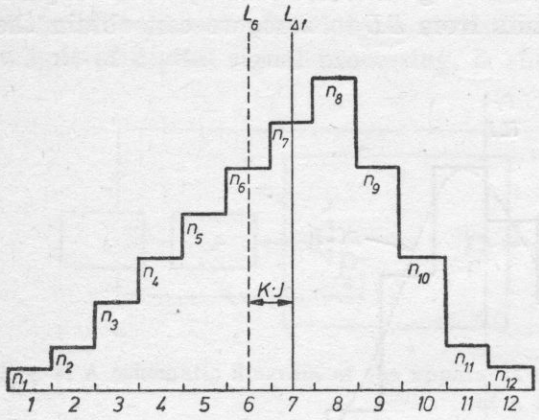

Fig. 6. An example of the distribution histogram with the marked quantities $L_{\Delta f}$, L_6, $n_1, \ldots, n_{12}$

$$K = \frac{1}{N}[(n_7 - n_5) + 2(n_8 - n_4) + 3(n_9 - n_3) + 4(n_{10} - n_2) + 5(n_{11} - n_1) + 6n_{12}];$$

$$L_{\Delta f} = L_6 + KJ = L_6 + K5 \quad [\text{dB}]; \tag{20}$$

$$R = \sqrt{\frac{1}{N}[(n_7 + n_5) + 4(n_8 + n_4) + 9(n_9 + n_3) + 16(n_{10} + n_{12}) + 25(n_{11} + n_1) + 36n_{12}] - K^2};$$

$$\sigma_{\Delta f} = RJ = R5 \quad [\text{dB}], \tag{21}$$

where $N = n_1 + n_2 + \ldots + n_{12}$ – the summary number of countings of the statistical analyser over a given frequency band Δf (the particular bands Δf, into which the frequency response of the room was divided, corresponded to 1/3 octave bandwiths); $n_1, n_2, \ldots, n_{12}$ – the number of countings in successive channels of the statistical analyser for a given band Δf; L_6 – the value of intensity level corresponding to channel 6 of the statistical analyser, J – channel unit equal to 1/10 of the value of the dynamics of the potentiometer used (in the present case $J = 5$ dB), $L_{\Delta f}$ – the mean value of sound intensity level of the frequency response, determined in the band Δf; $\sigma_{\Delta f}$ – the standard deviation of the frequency response from its mean value $L_{\Delta f}$, determined in the band Δf.

In order to evaluate qualitatively the degree of deviation of histograms obtained from a histogram corresponding to a normal distribution, values of the asymmetry coefficient A, defined by formula (22), were determined for them,

$$A = \frac{E[(L - L_{\Delta f})^3]}{\sigma^3} = \frac{\mu_3}{\sigma_3}, \tag{22}$$

where $E[]$ – the symbol of the mathematical expectation, μ_3 – the moment of the third order with respect to the mean value $L_{\Delta f}$.

For a symmetrical histogram form (i.e. for a normal distribution), this coefficient takes a zero value.

Values of the parameters $L_{\Delta f}$, $\sigma_{\Delta f}$ and A were determined by numerical calculations using for this purpose a specially constructed Fortran IV programme [8]. In addition the quantities F, defined by formula (1), and F_s, defined by formula (2), were also determined for all the cases under study.

4. Analysis of the measurement results

Fig. 7 shows as an example chosen sections of the behaviour of frequency responses recorded in the rooms under study and the corresponding histograms of sound intensity level change distribution.

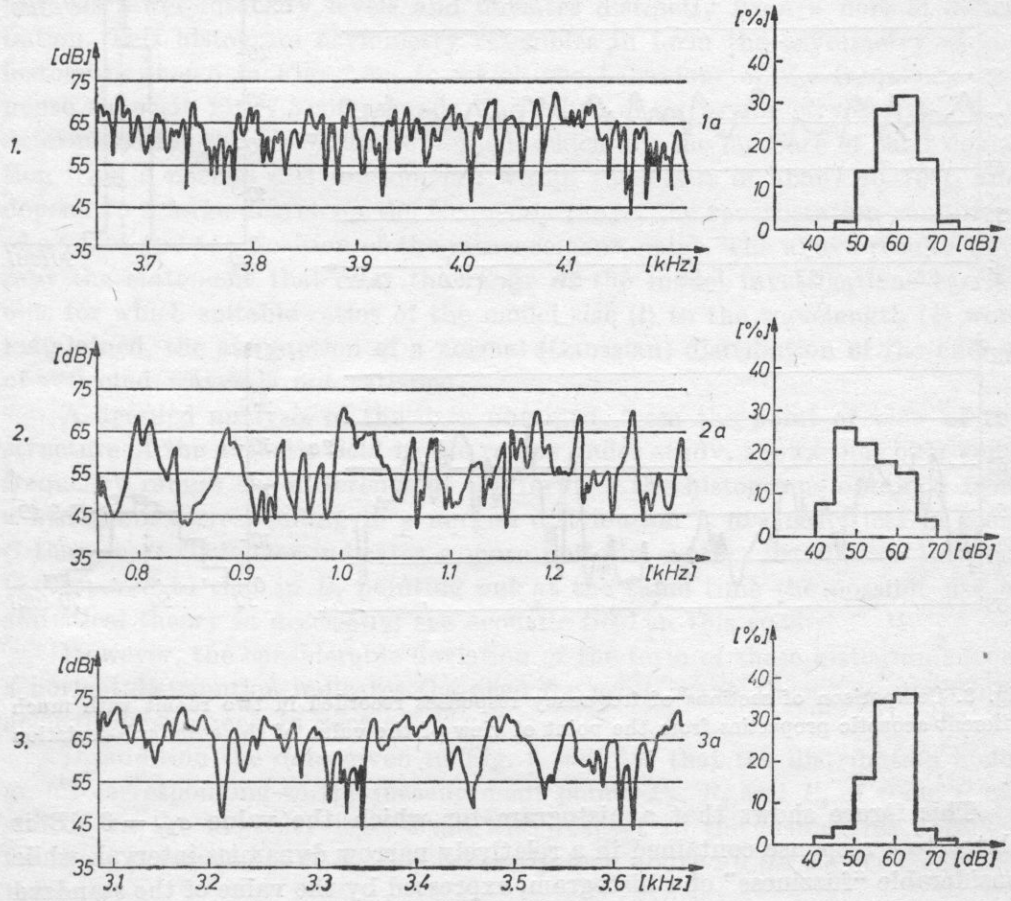

Fig. 7. Sections of frequency response curves and the corresponding distribution histograms, recorded in rooms with various acoustic properties

It is seen in Fig. 7 that these histograms are related in an interesting way to the character of the behaviour of the frequency response of the room. Thus, in a case when the behaviour of this response is close to the random behaviour (Fig. 7.1), the corresponding histogram takes a form corresponding in approximation to a normal distribution (Fig. 7.1*a*). The histogram shown in Fig. 7.2*a* corresponds to the behaviour of the response with maxima distinct on the amplitude scale (Fig. 7.2), while the histogram in the form shown in Fig. 7.3*a* is related to the response with clearly distinct minima (Fig. 7.3).

In addition it should be noted that the form of a distribution histogram also gives interesting information on the magnitude of dispersion of the frequency response of a room, whose measure is the value of the mean standard deviation, graphically illustrated in Fig. 8.

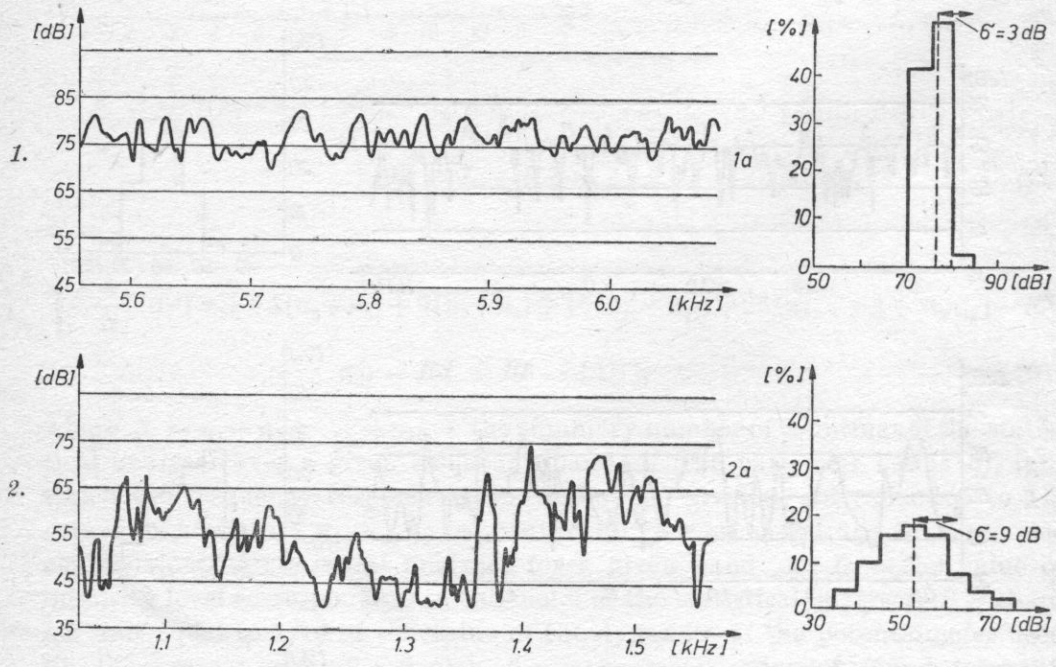

Fig. 8. Comparison of sections of frequency responses recorded in two rooms with much different acoustic properties from the point of view of the value of the standard deviation

This figure shows that a histogram for which the value $\sigma_{\Delta f} = 3$ dB is related to a response contained in a relatively narrow dynamics interval, while considerable "fuzziness" of a histogram, expressed by the value of the standard deviation $\sigma_{\Delta f} = 9$ dB corresponds to a response with large dispersion.

In order to analyse the form of the probability density function for the frequency responses under study, recorded in the rooms mentioned above, histograms of intensity level change probability distribution in successive 1/3 octave bands (Δf), within the range 630–8000 Hz, were plotted for these responses and the mean values of these levels ($L_{\Delta f}$) and the standard deviation ($\sigma_{\Delta f}$) calculated. The relatively high range of the frequencies considered resulted from the fact that the model investigations carried out required that a suitable ratio of the wavelength to the model size should be maintained. Some of these histograms, obtained for the considered measurement points of the damped room B (—) and the undamped room C (– – –), are shown as an example in Fig. 9.

From analysis of the form of the histograms shown in Fig. 9, it can be stated in general that the probability distribution of sound intensity level changes in the frequency response of a room indicates considerably asymmetry towards lower intensity levels and deviates distinctly from a normal distribution. This histogram asymmetry resembles in form the asymmetry of the histogram shown in Fig. 7.3*a*, to which the behaviour of the frequency response shown in Fig. 7.3 corresponds. The values of the asymmetry coefficient A determined for the histograms obtained, which are the measure of their deviation from a normal distribution, fall within the limits of about 40–70% and depend to a large degree on the frequency range, the reverberation conditions of a room and the position of the measurement point. The above results warrant the statement that over the range of the model investigations carried out, for which suitable ratios of the model size (l) to the wavelength (λ) were maintained, the assumption of a normal (Gaussian) distribution of the energy of reflected waves is not satisfied.

A detailed analysis of the data obtained, from the point of view of the structure of the acoustic field in the rooms under study, shows that over some frequency ranges the difference of the form of the histograms obtained from a histogram corresponding to a normal distribution is distinctly less in room C than in B. This fact indicates a more uniform energy distribution in room C compared to that in B, pointing out at the same time the possible use of statistical theory in describing the acoustic field in this room.

However, the considerable deviation of the form of these histograms from a normal distribution indicates the need for using wave theory in describing acoustic phenomena in rooms.

In addition the data given in Fig. 9 indicate that the distribution histograms corresponding to the measurement points P_2, P_3 and P_4 of room C are shifted on the intensity level scale with respect to the histograms obtained for those points in room B. This is clearly seen above all for higher frequency bands.

This effect results from the existence of different reverberation conditions

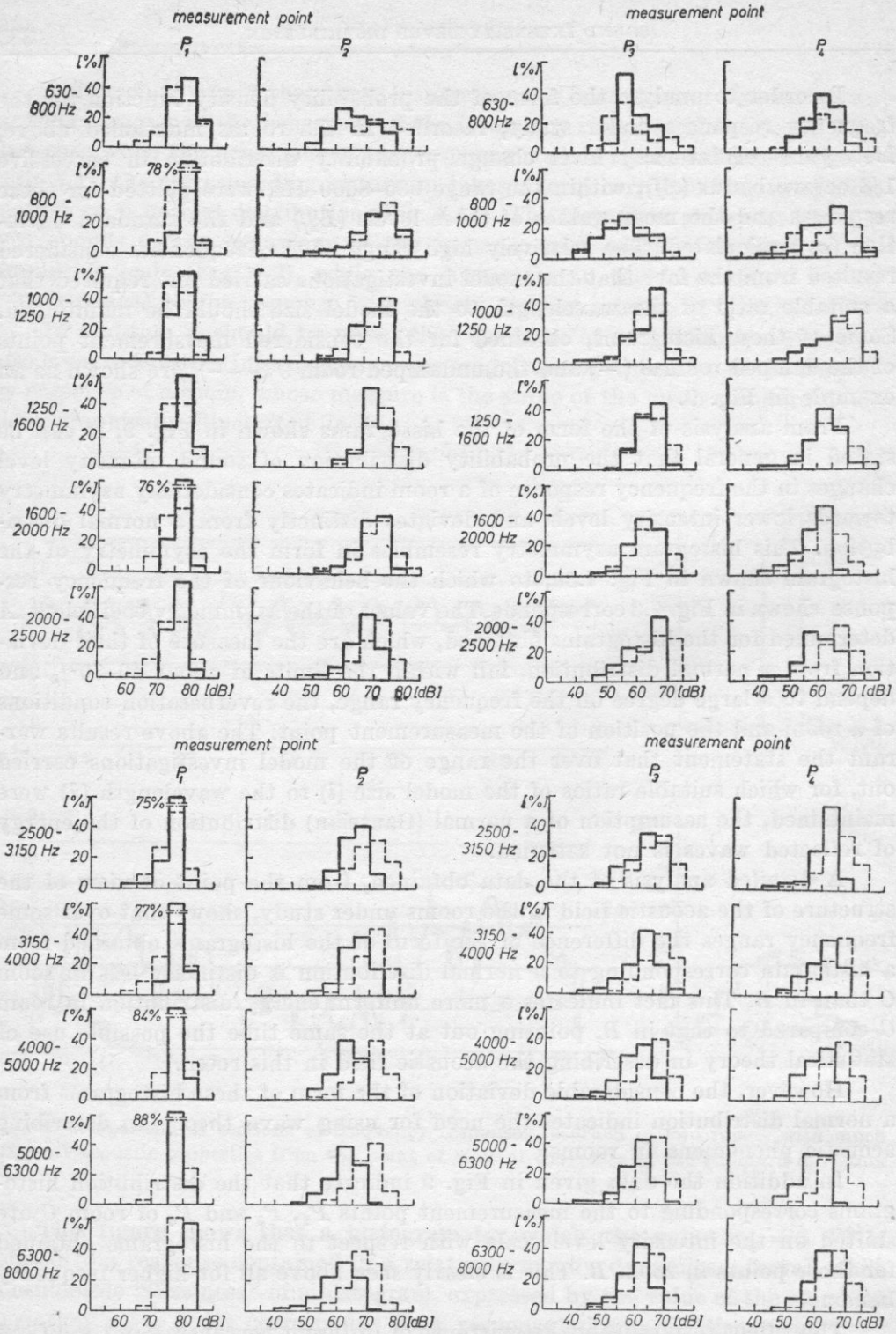

Fig. 9. Histograms of sound intensity level change distribution of frequency responses for successive 1/3 octave bands, measured at the measurement points P_1, P_2, P_3 and P_4 in room B (———) and room C (– – –)

in these rooms, on which the resultant value of sound intensity level is known to depend.

Comparison of the histograms obtained in the rooms under study, from the point of view of their "fuzziness", whose measure is the value of the standard deviation, indicates that the histograms for room C are more "fuzzy" than those for room B. In addition the change in the outline of these histograms, which is interesting with changes in the acoustical properties of the room, for some frequency bands and some measurement points represents a definite change in the distribution of maxima and minima of the frequency responses of the room, as was already mentioned in discussing Fig. 7.

Comparison of the mean values of the level $L_{\Delta f}$ of the frequency responses of rooms B and C in successive 1/3 octave bands is shown jointly in Fig. 10, line 1, whereas the values of the standard deviation $\sigma_{\Delta f}$ corresponding to these responses and determined in these bands are given in line 2. In addition the so-called irregularity density F[1], whose behaviour is shown in Fig. 10, line 3, was also calculated for these responses.

The mean values of the reverberation time T and the parameters $L_{\Delta f}$, $\sigma_{\Delta f}$, F and F_s, measured in rooms B and C at the measurement points P_1, P_2, P_3 and P_4, are given jointly in Table I.

In addition to investigations carried out in parallel-piped rooms B and C, analogous measurements were also carried out in two coupled rooms D and E, which differ from each other with the value of the coupling coefficients Q_{I} and Q_{II}, defined as

$$Q_{\mathrm{I}} = \frac{S_0}{a_{\mathrm{I}} S_{\mathrm{I}} + S_0}; \tag{23}$$

$$Q_{\mathrm{II}} = \frac{S_0}{a_{\mathrm{II}} S_{\mathrm{II}} + S_0}; \tag{24}$$

where Q_{I} – the coefficient of coupling the volume V_{I} with the volume V_{II}; Q_{II} – the coefficient of coupling the volume V_{II} with the volume V_{I}; a_{I}, a_{II} – the absorption coefficients of the volumes V_{I} and V_{II}; S_{I}, S_{II} – the surface areas of the walls of the volumes V_{I} and V_{II}: S_0 – the surface area of the coupling opening.

In the case of the coupled room D, part of the surface enclosing the volume V_{I} was covered with absorbing material (see Fig. 11), thus achieving, despite the different volumes V_{I} and V_{II}, close values of the acoustic coupling coefficients Q_{I} and Q_{II}, respectively: $Q_{\mathrm{I}} = 0.22$; $Q_{\mathrm{II}} = 0.24$. In turn, in the case of room E the surfaces enclosing the volumes V_{I} and V_{II} were made of the

[1] The author distinguishes between the so-called irregularity density of the frequency response, expressed by formula (1) and designated as F [dB/Hz], and the notion of dispersion of this response, whose measure is the quantity $\sigma_{\Delta f}$ [dB], expressed by formula (21).

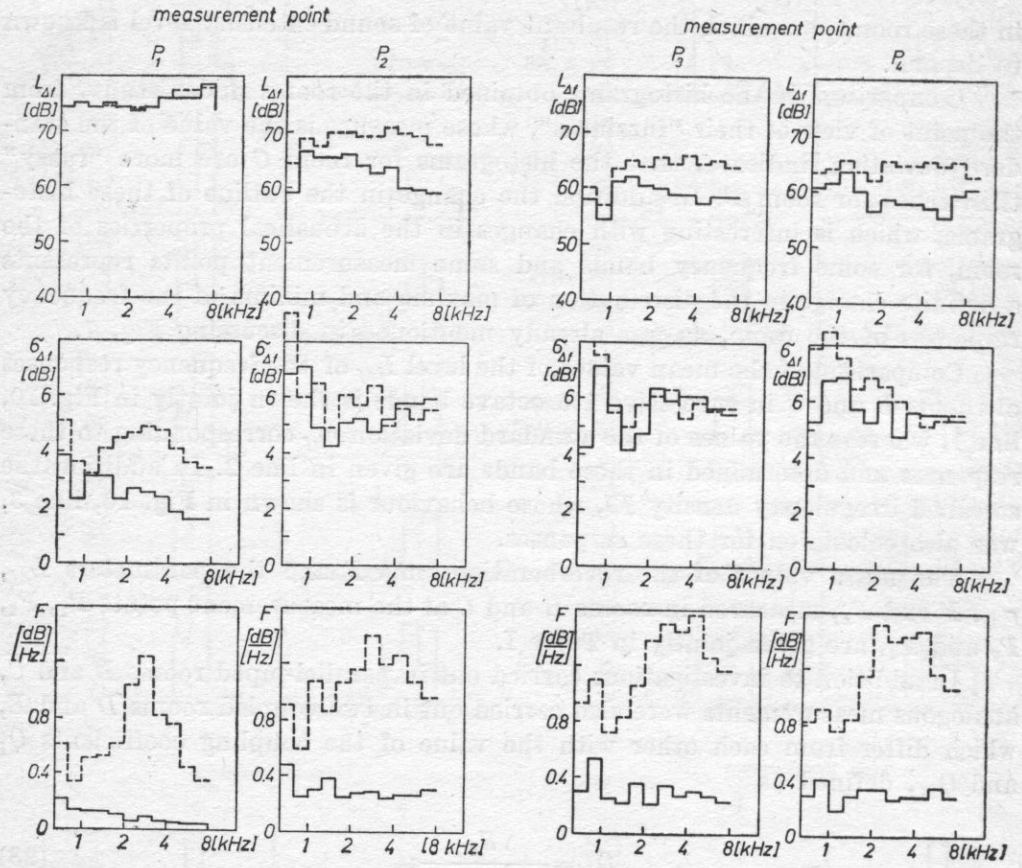

Fig. 10. Behaviour of the mean values of the intensity level $L_{\Delta f}$, the standard deviation $\sigma_{\Delta f}$ and the irregularity density F, determined for successive 1/3 octave bands of frequency responses, as recorded at the points P_1, P_2, P_3 and P_4 in room B (———) and room C (– – –)

same material with the mean absorption coefficient $\alpha \simeq 0.05$, effecting as a result a double increase in the coupling coefficient of the volume $V_{\mathrm{I}}(Q_{\mathrm{I}} = 0.47)$ compared with the coupling coefficient of the volume V_{II} $(Q_{\mathrm{II}} = 0.24)$.

The distribution of the absorbing materials and the position of measurement points in the coupled rooms are shown in Fig. 11. Fig. 12 shows as an example a comparison of sound intensity level distribution histograms for sucessive 1/3 octave bands of frequency responses obtained at the points $P_{2.\mathrm{I}}$ and $P_{2.\mathrm{II}}$, which fall in the volumes V_{I} and V_{II} of the coupled rooms D and E. These data show that the distribution histograms for the coupled room D are displaced on the level scale with respect to the histograms obtained for room E. This displacement clearly depends on the frequency band considered, with, both for the measurement point $P_{2.\mathrm{I}}$ and $P_{2.\mathrm{II}}$, above 2000 Hz, histograms for room E being displaced towards higher levels.

On the basis of the asymmetry coefficients determined for these histo-

Table I. The mean values of the reverberation time T and the parameters $L_{\Delta f}$, $\sigma_{\Delta f}$, F and F_s, obtained in rooms B and C, at the measurement points P_1, P_2, P_3 and P_4 (with averaging carried out over the frequency range 630–8000 Hz)

Measurement point	Room B (damped)					Room C (undamped)				
	T	$L_{\Delta f}$	$\sigma_{\Delta f}$	F	F_s	T	$L_{\Delta f}$	$\sigma_{\Delta f}$	F	F_s
	[s]	[dB]	[dB]	[dB/Hz]	[dB/Hz]	[s]	[dB]	[dB/Hz]	[dB/Hz]	[dB/Hz]
P_1 ($x = 5, y = 0, z = 0$)	–	75	2.6	0.08	–	–	75	4	0.65	–
P_2 ($x = 100, y = 0, z = 0$)	0.2	61	5.6	0.28	0.25	0.7	67	6	0.95	0.98
P_3 ($x = 112, y = 20, z = 32$)	0.22	58	5.6	0.3	0.3	0.75	62	5.8	1.05	1.05
P_4 ($x = 135, y = 30, z = -60$)	0.22	58	5.6	0.3	0.3	0.75	63	6.0	1.02	1.05

Table II. The mean values of the reverberation time T and the parameters $L_{\Delta f}$, $\sigma_{\Delta f}$, F and F_s, obtained in the coupled rooms D and E, at the measurement points $P_{2.\mathrm{I}}$ and $P_{2.\mathrm{II}}$ (with averaging carried out over the frequency range 630–8000 Hz)

Measurement point	Coupled room D					Coupled room E				
	T	$L_{\Delta f}$	$\sigma_{\Delta f}$	F	F_s	T	$L_{\Delta f}$	$\sigma_{\Delta f}$	F	F_s
	[s]	[dB]	[dB]	[dB/Hz]	[dB/Hz]	[s]	[dB]	[dB]	[dB/Hz]	[dB/Hz]
$P_{2.\mathrm{I}}$($x = 38, y = 20, z = 32$)	0.35	57	6.5	0.20	0.49	0.6	63	5.7	0.57	0.84
$P_{2.\mathrm{II}}$($x = 100, y = 0, z = 0$)	0.55	56	5.8	0.58	0.77	0.7	63	5.7	0.68	0.98

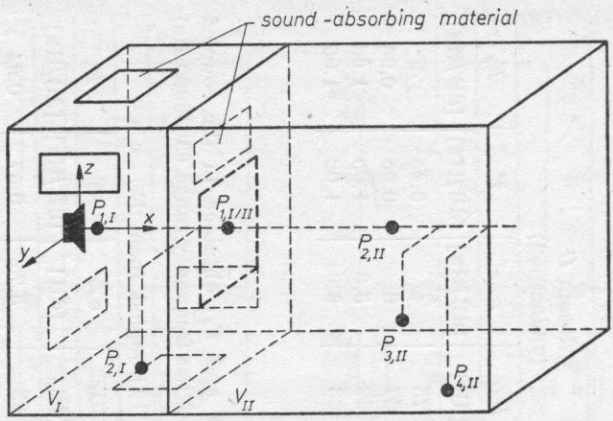

Fig. 11. The distribution of absorbing materials and the position of the measurement points $P_{2.I}$ ($x = 38$, $y = 20$, $z = 32$) and $P_{2.II}$($x = 100$, $y = 0$, $z = 0$) in the coupled room D

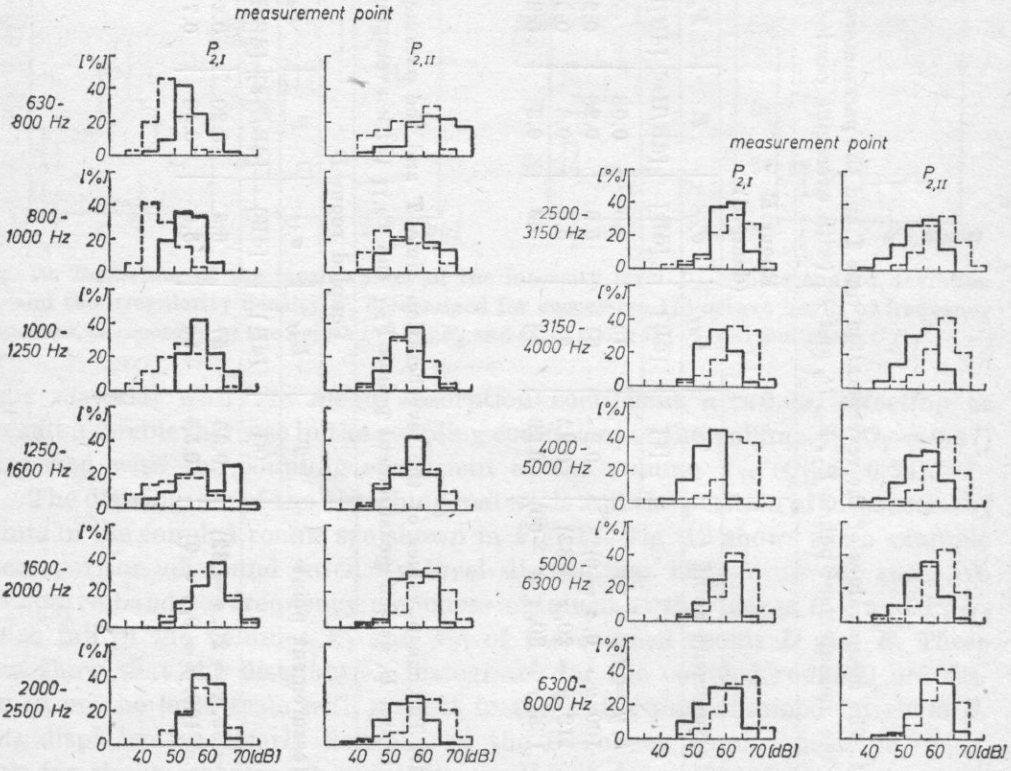

Fig. 12. Histograms of sound intensity level change distribution of frequency responses for successive 1/3 octave bands, measured at the measurement points $P_{2.I}$ and $P_{2.II}$ in the coupled rooms D (———) and E (– – –)

grams, it can be stated in general that, similarly to rooms B and C, in the coupled rooms the sound intensity level change distribution of the frequency responses analysed deviates from a normal one. Interesting information on the magnitude of dispersion of the frequency responses of rooms D and E is contained in the "fuzziness", various in form, of particular histograms. Comparison of the mean values of intensity level, $L_{\Delta f}$, for the frequency responses of the coupled rooms D and E the values of the standard deviation corresponding to these levels, and also values of the parameter F for successive 1/3 octave bands of these responses, are given in Fig. 13. In turn the mean values of the parameters $L_{\Delta f}$, $\sigma_{\Delta f}$ and F, measured at the points $P_{2.\mathrm{I}}$ and $P_{2.\mathrm{II}}$ of the coupled rooms D and E, are given jointly in Table II.

It is seen in Fig. 13 that in the volume V_{I} (measurement point $P_{2.\mathrm{I}}$ of the coupled rooms D and E) there is a quite large differentiation in the behaviour of the values of the parameters $L_{\Delta f}$ and F. In turn, in the volume V_{II} (measurement point $P_{2.\mathrm{II}}$), which is the same in terms of size and interior decoration for rooms D and E, the difference between the behaviour of the value of the coefficient $L_{\Delta f}$ for these rooms is still quite large, whereas the behaviours of the coefficient F in these rooms are quite close. The values of the standard deviation $\sigma_{\Delta f}$ for rooms D and E do not show unambiguous differences either in the volume V_{I} or in V_{II}, but they are different for these volumes in the character of the behaviour as a function of frequency.

In conclusion, it should be stressed that apart from the model investigations carried out, it is essential to verify experimentally the assumption of a random distribution of the energy of reflected waves in real rooms with large volume.

5. Conclusions

1. A detailed analysis of ample experimental material shows that histograms of sound intensity level change distribution of the analysed frequency responses obtained for the rooms under study are different from a normal distribution within the limits of the asymmetry coefficient up to as much as 70%. This difference depends to a large extent on the reverberation conditions of the room, the frequency band and the position of the measurement point. The results of the present experimental investigations thus permit the statement that in the range of model investigations the assumption of a normal (Gaussian) distribution of the energy of reflected waves is not satisfied.

2. The forms of histograms describing the sound intensity level distribution of frequency responses recorded at chosen measurement points and the corresponding values of the asymmetry coefficients A permit the establishment of a criterion for selecting an adequate (statistical or wave) theory for description of acoustic phenomena in a room. It can be assumed that the distribution histograms which are close to a normal distribution within the

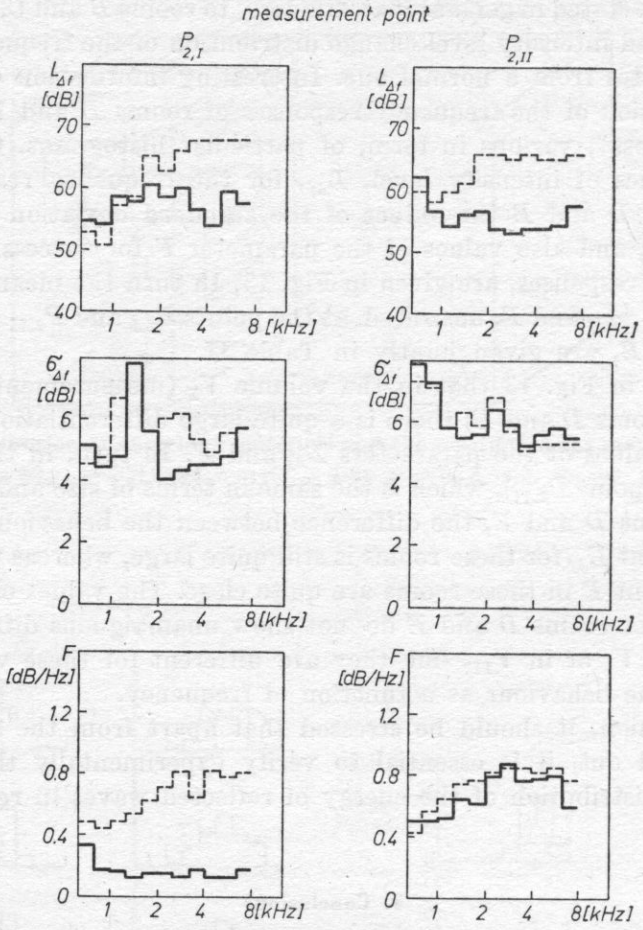

Fig. 13. Behaviour of the mean values of the intensity level $L_{\Delta f}$, the standard deviation $\sigma_{\Delta f}$ and the irregularity density F, as determined for successive 1/3 octave bands of frequency responses recorded at the points $P_{2,I}$ and $P_{2,II}$ in the coupled rooms D (———) and E (— — —).

limits of a small value of A represent well a uniform distribution of the energy of the acoustic field in a room, suggesting at the same time the possibility of describing the field by statistical theory. In turn the large deviation of the forms of these histograms from a normal distribution, which is expressed by a high value of A, suggests the need for analysis of acoustic phenomena in a room by means of wave theory.

3. The mean value of the standard deviation from the value $L_{\Delta f}$ for frequency responses, determined in the reverberant field of the rooms considered, falls within the limits 5.6–6 dB and is in good agreement with an analogous quantity defining the irregularity of the distribution of acoustic energy in a room, of about 5.6 dB, as obtained in paper [9]. It should be added that

this value corresponds to the mean change in the intensity level of the spectral components of the sound spectrum analysed in paper [8].

4. The results of measurements of the parameter F of frequency responses recorded in rooms B and C are in good agreement with those of calculations of the parameter F_s, determined from formula (2). However, in the coupled rooms D and E measurements of the parameter F give in all cases values much lower than those of F_s.

The investigation results given above and their analysis indicate that interesting information on the behaviour of the frequency response of a room can be gained by analysing its statistical parameters. It can be expected that, apart from the distribution histograms and the corresponding mean values, standard deviations and asymmetry coefficients, determined above for frequency responses under study, determination for these responses of other additional parameters, based on statistical moments of higher orders, would permit an even more accurate description of the behaviour of the frequency response, and thus a fuller evaluation of the structure of the acoustic field in a room.

References

[1] R. H. Bolt, R. W. Roop, *Frequency response fluctuations in rooms*, J. Acoust. Soc. Am., **22**, 280–289 (1950).

[2] Brüel-Kjaer, *Statistical distribution analyser type 4420 (instruction and application)*.

[3] W. T. Chu, *Statistical properties of energy spectral response as a function of direct-to-reverberant energy ratio*, J. Acoust. Soc. Am., **68**, 1208–1210 (1980).

[4] H. G. Diestel, *Zur Schallausbreitung in reflexionsarmen Raeumen*, Acustica, **12**, 113–118 (1962).

[5] K. J. Ebeling, *Influence of direct sound on the fluctuations of the room spectral response*, J. Acoust. Soc. Am., **68**, 1206–1207 (1980).

[6] J. J. Jetzt, *Critical distance measurement of rooms from the sound energy spectral response*, J. Acoust. Soc. Am., **65**, 1204–1211 (1979).

[7] H. Kuttruff, R. Thiele, *Über die Frequenzabhängigkeit des Schalldrucks in Räumen*, Acustica, **4**, 614–617 (1954).

[8] E. Ozimek, *Investigations of changes in the spectral structure of sound propagating in an enclosure* (in Polish), Scientific Publications, Adam Mickiewicz University, Poznań 1977.

[9] M. R. Schroeder, *Die Statistiche Parameter der Frequenzkurven von Grossen Räumen*, Acustica, **4**, 594–600 (1954).

[10] M. R. Schroeder, *Frequency-correlation functions of frequency responses in rooms*, J. Acoust. Soc. Am., **34**, 1819–1823 (1962).

[11] M. R. Schroeder, *Eigenfrequenzstatistik und Anregnungsstatistik in Räumen*, Acustica, **4**, 456–468 (1954).

[12] M. R. SCHROEDER, H. KUTTRUFF, *On frequency response curves in rooms comparison of experimental, theoretical and Monte Carlo results for the average frequency spacing between maxima*, J. Acoust. Soc. Am., **34**, 76–80 (1962).

[13] R. V. WATERHOUSE, *Statistical properties of reverberant sound fields*, J. Acoust. Soc. Am., **43**, 1436–1444 (1968).

[14] E. C. WENTE, *Characteristics of sound transmission in rooms*, J. Acoust. Soc. Am., **7**, 123–131 (1935).

Received on 20 June, 1983

ARCHIVES OF ACOUSTICS
9, 3, 349-354 (1984)

ANALYSIS OF BROAD-BAND PIEZOELECTRIC SANDWICH TRANSDUCER WITH PERFORATED STRUCTURE

LIN CHONG-MAO, HOU LI-QI, YING CHUNG-FU

Institute of Acoustics*, Academia Sinica, Peking

1. Introduction

Pre-stressed piezoelectric sandwich transducers are used widely as sonic source for many low frequency ultrasonic applications, notably in the fields of macrosonics sand sonar. For certain applications a broader bandwidth is necessary. The sandwich transducer with perforated structure developed by us is formed by drilling holes longitudinally in the radiating head, and has been shown experimentally to possess a bandwidth approximately double that of a conventional nonperforated transducer, while its electroacoustic efficiency remains almost undeteriorated [1].

In this paper a theoretical model for the broadband structure is proposed. The frequency characteristics of the input electrical admittance of the transducer and the input mechanical impedance of the radiating head loaded by water, are calculated both as functions of the relative cross-section α of the bored part and the relative depth of the holes β of the radiating head. Some theoretical results are compared with measured ones, the two fairly well agree.

2. Theoretical consideration

A sandwich transducer with perforated structure is shown in Fig. 1a. It is composed of a backing block (1); two piezoelectric ceramics (2), (4); an electrode (3); a radiating head with perforated structure (5), (6) and a thin cover plate (7). These sections are connected mechanically in series. A bolt for pre-stressing is ignored. Parts (5), (6) and (7) are considered to form a mechanical "transformer section". The backing block and the radiating head are electrically connected, and a constant voltage E is applied between the electrode and the backing block, so that the two ceramic discs are connected electrically in parallel. The transducer is loaded to the right. By making the usual

* Work done while at Institute of Physics.

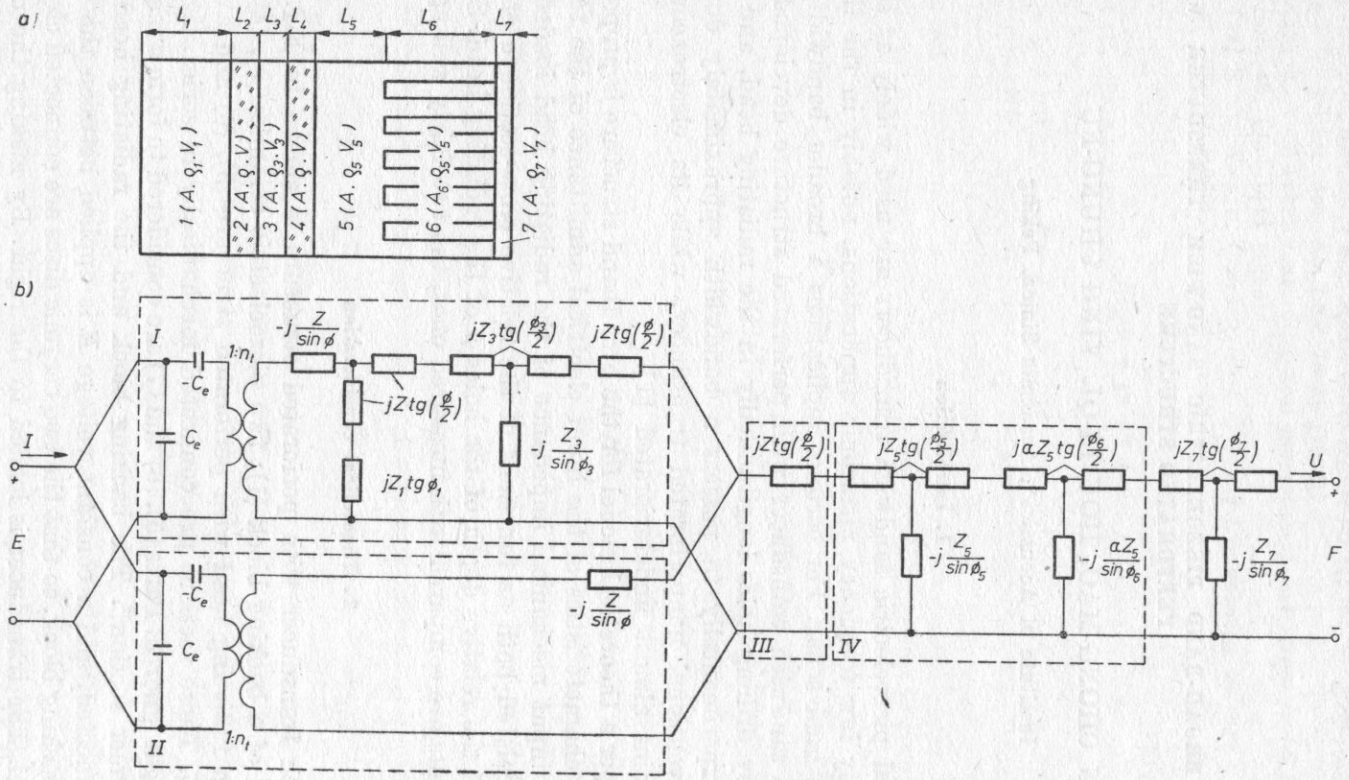

Fig. 1a. Transducer with perforated structure

1 – backing block; *5, 6* – radiating head; *2, 4* – ceramics; *7* – cover plate; *3* – electrode

Fig. 1b. Equivalent electro-mechanical network of the transducer

one-dimensional approximation and neglecting the mechanical and dielectric losses, the equivalent electromechanical network of the transducer is given in Fig. 1*b*. In this model of analysis, the radiating section with perforated structure is treated as two cascade acoustic transmission lines of different cross-section A and A_6, A_6 being A minus the total area bored out. It is represented in Fig. 1*b* by two cascade T — networks in the dash line block IV.

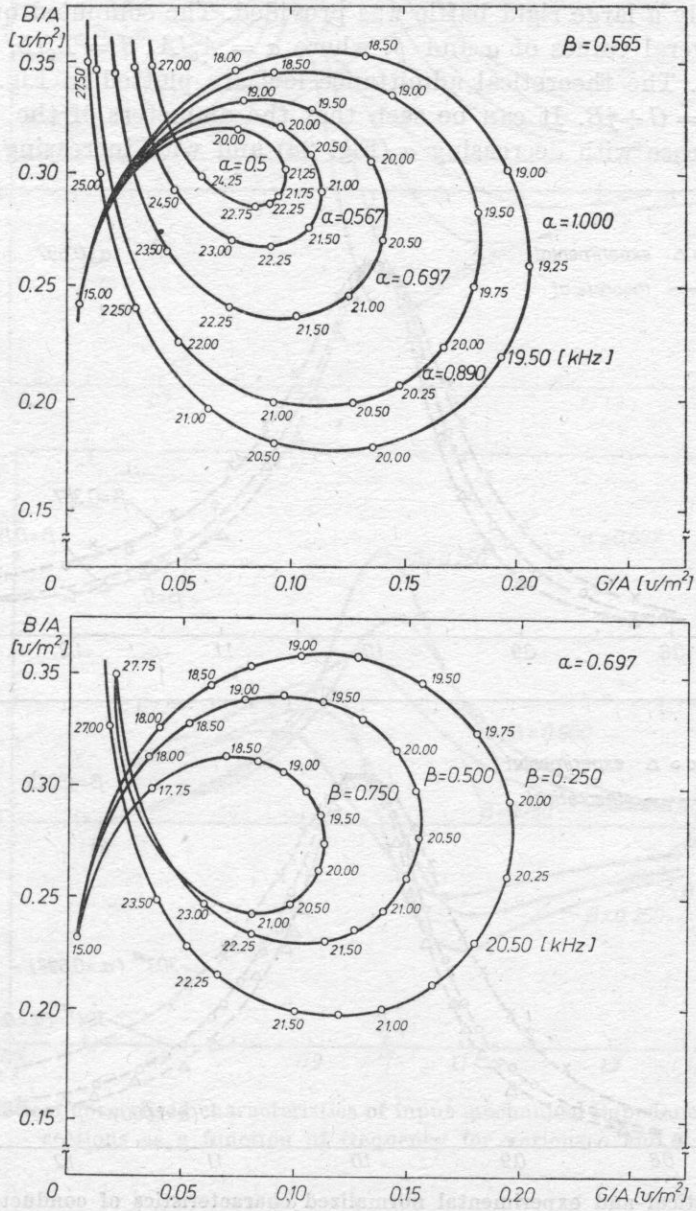

Fig. 2. Theoretical admittance loci of transducers for various α and β

3. Results and discussion

A computer program was effected to calculate from the network in Fig. 1*b* the electrical admittance at the electrical terminal of the transducer and the mechanical impedance looking into the "transformer section". These two quantities are related to the acoustical bandwidth of the transducer. The radiating face is supposed to be rigid and set in an infinite rigid baffle in water; experimentally a large rigid baffle was provided. The computed quantities are given for several values of α and β, where $\alpha = A_6/A$, $\beta = L_6/L$, $L = L_5 + L_6$ (see Fig. 1*a*). The theoretical admittance loci are plotted in Fig. 2*a* and 2*b*, in which $Y = G + jB$. It can be seen that the diameters of the "admittance circles" decrease with decreasing α (Fig. 2*a*) and with increasing β (Fig. 2*b*),

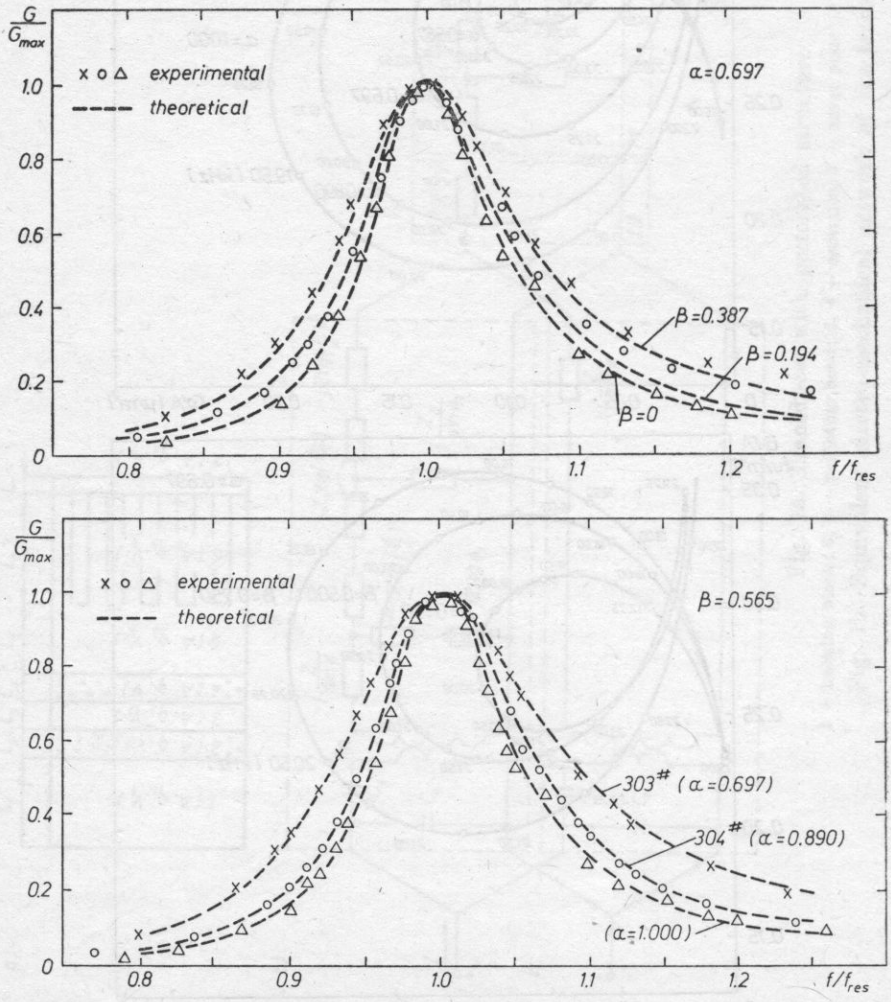

Fig. 3. Theoretical and experimental normalized characteristics of conductance of transducers as a function of frequency for various α and β

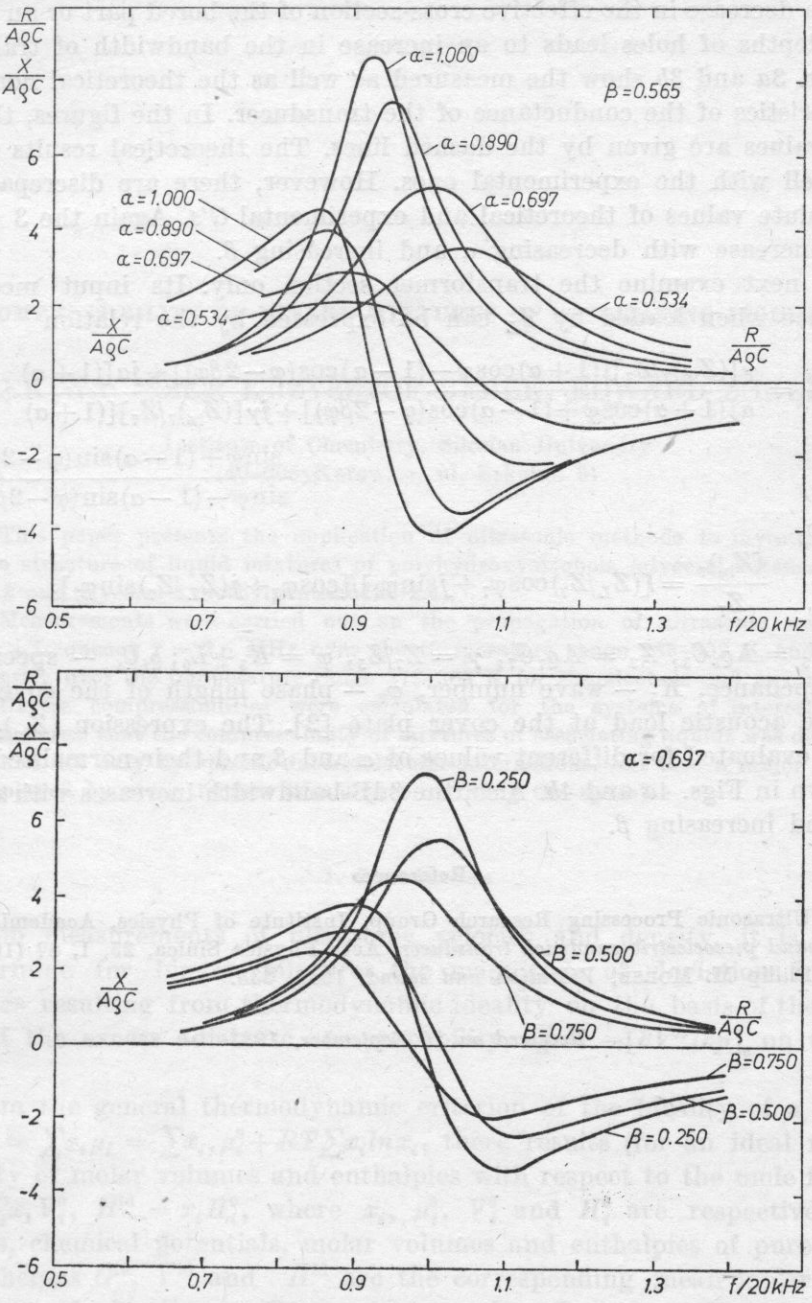

Fig. 4. Theoretical normalized characteristics of input mechanical impedance of transformer sections as a function of frequency for various α and β.

that is, a decrease in the effective cross-section of the bored part or an increase in the depths of holes leads to an increase in the bandwidth of transducer.

Figs. 3*a* and 3*b* show the measured as well as the theoretical normalized characteristics of the conductance of the transducer. In the figures, the theoretical values are given by the dashed lines. The theoretical results seem to agree well with the experimental ones. However, there are discrepancies in the absolute values of theoretical and experimental *G's*. Again the 3 dB-bandwidths increase with decreasing α and increasing β.

We next examine the transformer section only. Its input mechanical impedance when loaded by Z_L can be expressed by the relation

$$\frac{(Z_{\text{in}})_5}{Z_5} = \frac{\gamma[(Z_{\text{in}})_7/Z_7][(1+\alpha)\cos\varphi-(1-\alpha)\cos(\varphi-2\beta\varphi)]+j\alpha[(1+\alpha)}{\alpha[(1+\alpha)\cos\varphi+(1-\alpha)\cos(\varphi-2\beta\varphi)]+j\gamma[(Z_{\text{in}})_7/Z_7][(1+\alpha)} \times$$

$$\times \frac{\sin\varphi+(1-\alpha)\sin(\varphi-2\beta\varphi)}{\sin\varphi-(1-\alpha)\sin(\varphi-2\beta\varphi)]},$$

in which,

$$\frac{(Z_{\text{in}})_7}{Z_7} = [(Z_L/Z_7)\cos\varphi_7+j\sin\varphi_7]/[\cos\varphi_7+j(Z_L/Z_7)\sin\varphi_7],$$

where $Z_5 = A\varrho_5 C_5$, $Z_7 = A\varrho_7 C_7$, $\gamma = Z_7/Z_5$, $\varphi = K_5+L_6$; $\varrho_i C_i$ – specific acoustic impedance, K_5 – wave number, φ_7 – phase length of the cover plate, Z_L – the acoustic load at the cover plate [2]. The expression $(Z_{\text{in}})_5 = R+jX$ is evaluated for different values of α and β and their normalized values are shown in Figs. 4*a* and 4*b*. Also, the 3dB-bandwidth increases with decreasing α and increasing β.

References

[1] Ultrasonic Processing Research Group, Institute of Physics, Academia Sinica, *A broad band piezoelectric sandwich transducer*, Acta Physica Sinica, **25**, 1, 87 (1976).

[2] Philip M. MORSE, *Vibration and sound*, 1948, 333.

Received on 20 September, 1983

ARCHIVES OF ACOUSTICS
9, 3, 355-362 (1984)

COMPRESSIBILITY OF BINARY MIXTURES OF ASSOCIATING LIQUIDS

MAREK WACIŃSKI, KRZYSZTOF BEBEK, EDWARD ZORĘBSKI

Institute of Chemistry, Silesian University
(40–006 Katowice, ul. Szkolna 9)

This paper presents the application of ultrasonic methods to investigate the structure of liquid mixtures of polyhydroxyalcohols (glycerol-butanediol-1.3 and glycerol-2-methylpentanediol-2.4).

Measurements were carried out on the propagation of ultrasonic waves at a frequency $f = 2.5$ MHz over the temperature range 283–303 K and on density over the temperature range 273–303 K for the alcohols and mixtures.

Excess compressibilities were calculated for the systems of interest. It was shown that the compressibility of mixtures of associating liquids was determined not only by specific intermolecular interactions, but also a major role is played by steric factors (the degree of filling the space).

1. Introduction

From measurements of ultrasonic velocity and density, it is possible to determine for binary mixtures the magnitude of deviation from the properties resulting from thermodynamic ideality on the basis of the dependence of the excess adiabatic compressibility $\varkappa_S^E = -[\partial V^E/\partial p]_s$ on the mole fraction.

From the general thermodynamic criterion of the ideality of a mixture [1], $\bar{G}^{id} = \sum x_i \mu_i = \sum x_i \mu_i^0 + RT \sum x_i \ln x_i$, there results (for an ideal mixture) additivity of molar volumes and enthalpies with respect to the mole fraction: $\bar{V}^{id} = \sum x_1 V_i^0$, $\bar{H}^{id} = x_i H_i^0$, where x_i, μ_i^0, V_i^0 and H_i^0 are respectively mole fractions, chemical potentials, molar volumes and enthalpies of pure component; whereas $\bar{G}^{id}$, $\bar{V}^{id}$ and $\bar{H}^{id}$ are the corresponding mean molar quantities for an ideal mixture. Hence, taking, after ROTHHARDT'S proposal [2], enthalpy as the basic thermodynamic potential, for an ideal binary mixture

$$\bar{H}^{id} = x_1 H_1^0 + x_2 H_2^0,$$

$$\bar{\varkappa}^{id} = \left(\frac{\partial^2 \bar{H}^{id}}{\partial p^2}\right)_{\bar{s}} = x_1 \left(\frac{\partial^2 \bar{H}_1^0}{\partial p^2}\right)_{\bar{s}} + x_2 \left(\frac{\partial^2 H_2^0}{\partial p^2}\right)_{\bar{s}} = x_1 \left(\frac{\partial V_1^0}{\partial p}\right)_{\bar{s}} + x_2 \left(\frac{\partial V_2^0}{\partial p}\right)_{\bar{s}}. \qquad (1.1)$$

Assuming that

$$\left(\frac{\partial^2 H_i^0}{\partial p^2}\right)_{\bar{s}} \approx \left(\frac{\partial^2 H_i^0}{\partial p^2}\right)_{s_i^0} = \varkappa_i^0 \tag{1.2}$$

the adiabatic compressibility of an ideal binary mixtures can be regarded as a quantity approximately additive with respect to the mole fraction

$$\varkappa^{\mathrm{id}} = x_1 \varkappa_1^0 + x_2 \varkappa_2^0. \tag{1.3}$$

The approximate character of this additivity results from the fact that $\bar{s} = \sum x_i s_i^0 - R \sum x_i \ln x_i \neq s_i^0$ and that despite the constant entropy of the whole mixture $s = \mathrm{const}$ in the process of compression and decompression, the constancy of the component entropies $s_i = \mathrm{const}$ is not ensured [3, 4].

It seems, however, that the approximation on which equation (1.3) is based, is satisfied sufficiently well for the deviation of binary mixture from thermodynamic ideality to be evaluated from excess adiabatic compressibility, defined as

$$\bar{\varkappa}_s^E = \bar{\varkappa}_s - \bar{\varkappa}_s^{\mathrm{id}} = \bar{\varkappa}_s - (x_1 \varkappa_1^0 + x_2 \varkappa_2^0). \tag{1.4}$$

2. Experimental part

Both glycerol (P.O.Ch. Gliwice, pure for analysis), 2-methylpentanediol-2.4 (BDH Chemicals Ltd., pure), and butanediol-1.3 (Koch-Light Laboratories Ltd, pure) were dehydrated by boiling under reduced pressure at a temperature of about 373 K.

The densities of mixtures and pure components were determined pycnometrically over the temperature range 273–303 K, at temperature stability of ± 0.05 K. To reduce the weight in air, the relation $\varrho = \varrho' + 0.0012\,(1 - \varrho'/\varrho^0)$ was used, where ϱ — absolute density of water, ϱ' — measured density. The dependence of density on temperature can be represented by the linear equation $\varrho = AT + B$, where A and B are constants determined by the least squares method. The density equations are listed in Table 1, where r — the correlation coefficient of the linear dependence of ϱ on T; x_2 — mole fraction of the diol.

The ultrasonic wave propagation at a frequency of 2.5 MHz in the solutions under study and its changes over the temperature range 283–303 K were measured by an ultrasonic pulse-phase interferometer (produced by Institute of Fundamental Technological Research, Polish Academy of Sciences) with accuracy of ± 0.05 per cent (Table 2, where x_2 — mole fraction of the diol).

Table 1

x_2	Glycerol-butanediol-1.3	
	ϱ [kg/m^3]	r
0.	$-6.2410\times10^{-1}T+1.4430\times10^{3}$	−0.9995
0.1020	$-6.0437\times10^{-1}T+1.4061\times10^{3}$	−0.9992
0.2035	$-6.0471\times10^{-1}T+1.3684\times10^{3}$	−0.9993
0.3046	$-6.2925\times10^{-1}T+1.3501\times10^{3}$	−0.9991
0.5054	$-6.2278\times10^{-1}T+1.2979\times10^{3}$	−0.9996
0.7045	$-6.2214\times10^{-1}T+1.2510\times10^{3}$	−0.9989
1	$-6.9167\times10^{-1}T+1.2037\times10^{3}$	−0.9994
	Glycerol-2-methylpentanediol-2.4	
0.0314	$-6.5545\times10^{-1}T+1.4273\times10^{3}$	−0.9989
0.0879	$-7.0780\times10^{-1}T+1.4173\times10^{3}$	−0.9996
0.1716	$-6.9645\times10^{-1}T+1.3791\times10^{3}$	−0.9954
0.2956	$-6.9524\times10^{-1}T+1.3282\times10^{3}$	−0.9960
0.4478	$-6.2032\times10^{-1}T+1.2531\times10^{3}$	−0.9948
0.6452	$-6.5025\times10^{-1}T+1.1981\times10^{3}$	−0.9317
0.8153	$-6.6247\times10^{-1}T+1.1616\times10^{3}$	−0.9960
1	$-6.1967\times10^{-1}T+1.1051\times10^{3}$	−0.9996

Table 2

u[m/s]

x_2	283.15 K	293.15 K	303.15 K
	Glycerol-butanediol-1.3		
0	1944.5	1920.1	1895.8
0.1020	1894.0	1869.6	1844.8
0.2035	1840.0	1819.3	1798.1
0.3046	1797.5	1773.7	1751.7
0.5054	1722.0	1696.2	1672.0
0.7045	1653.0	1626.4	1600.6
1	1573.0	1547.0	1519.0
	Glycerol-2-methylpentanediol-2.4		
0.0314	1906.4	1882.2	1858.2
0.0879	1850.8	1826.0	1801.3
0.1716	1781.0	1754.2	1728.4
0.2956	1667.8	1638.4	1610.0
0.4478	1568.5	1539.4	1510.5
0.6452	1470.0	1440.0	1410.0
0.8153	1411.2	1380.3	1350.0
1	1344.0	1311.0	1280.0

3. Discussion of the results and conclusions

The excess compressibilities calculated from equation (1.4) for the two systems under study: I — glycerol-butanediol-1.3 and II — glycerol-2-methylpentanediol-2.4, are shown in Figs. 1 and 2. Over the whole concentration

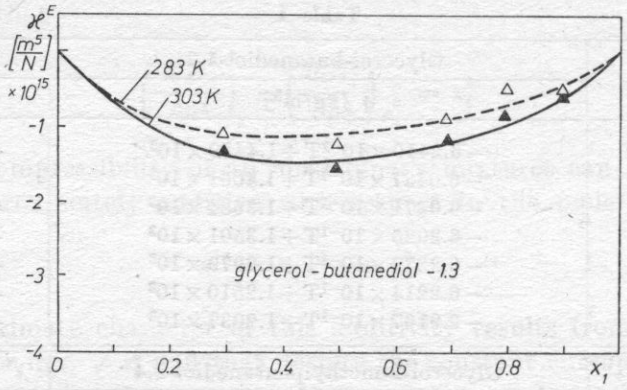

Fig. 1. Excess compressibility as a function of the mole fraction (calculated from equation (1.4)) for the glycerol-butanediol-1.3 system

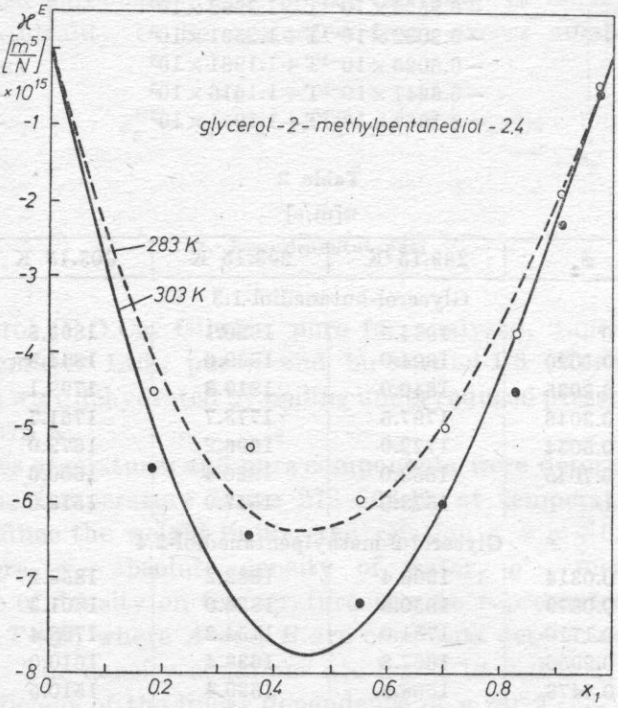

Fig. 2. Excess compressibility as a function of the mole fraction (calculated from equation (1.4)) for the glycerol-2-methylpentanediol-2.4 system

range the excess adiabatic compressibilities are negative. The components of the mixtures of interest are liquids of a high degree of association. Specific intermolecular interactions in the form of hydrogen bonds lead to the formation of incessantly disintegrating and reintegrating disturbed fragments of the

crystal structure (subject to translation and not separated by discontinuity boundaries), and also determine the response to mechanical stress [5–9]. The formation of intra- and intermolecular hydrogen bonds should in the case of mixtures of polyhydric liquids lead to the formation of relatively extensive clusters (increased degree of association).

On the basis of JACOBSON's model of intermolecular free path [14], the formation of complexes between the components of a mixture was repeatedly related in the literature [10, 11] to an increase in compressibility (positive excess compressibility), with complexes (associates) considered incompressible.

However, this assumption seems to be unwarranted, particularly in the case of multimers formed by hydrogen bonds. According to KUDRYAVTSEV [12] and KUCZERA [13], the acoustic wave propagation is not only an intermolecular effect. Particularly in the case of an extensive cluster, the transmission of an acoustic pulse within the cluster must occur at finite velocity. On the assumption that the pulse transmission along a hydrogen bond is faster than on a free path, it can be shown that association should cause an increase in the phase velocity and decreased compressibility ("stiffening" of the system). It can thus be concluded that negative excess compressibilities indicate stronger association in mixtures than in pure components.

Since in the case of the two mixtures one of the components is common to both (glycerol), whereas the two diols differ only in the number of methyl groups:

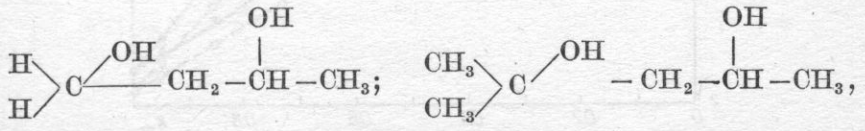

similar abilities to form hydrogen bonds (association) can be expected in the two systems. However, mixture II shows much greater negative compressibility, suggesting the possibility of the free space in the openwork structure of the cluster having been "blocked" by two additional methyl groups of 2-methylpentanediol-2.4. Thus, it can be stated that the compressibility of a liquid system is determined not only by specific intermolecular interactions, but also that a major role is played by steric factors.

In the case of the two mixtures, the excess compressibilities become more and more negative with increasing temperature (Figs. 1 and 2). This indicates the formation of increasingly firm clusters (more immune to the disturbing effect of thermal motion) in the mixtures compared to the clusters which form in the pure components. Fig. 3 shows the properties of mixture II at temperatures of 283 K and 303 K, based on the dependence of the coefficients of adiabatic compressibility of a real mixture, β_s, and an ideal one, β_s^{id}, on the concentration represented in volume fractions x_{v1} of glycerol. An increase in the di-

fference between β_s and β_s^{id} (the latter defined usually as $\beta_s^{id} = \sum x_{vi}\beta_{si}$ [4]) with increasing temperature, indicates more negative excess compressibilities while for two different temperatures $T_2 > T_1$ the "absolute" compre-

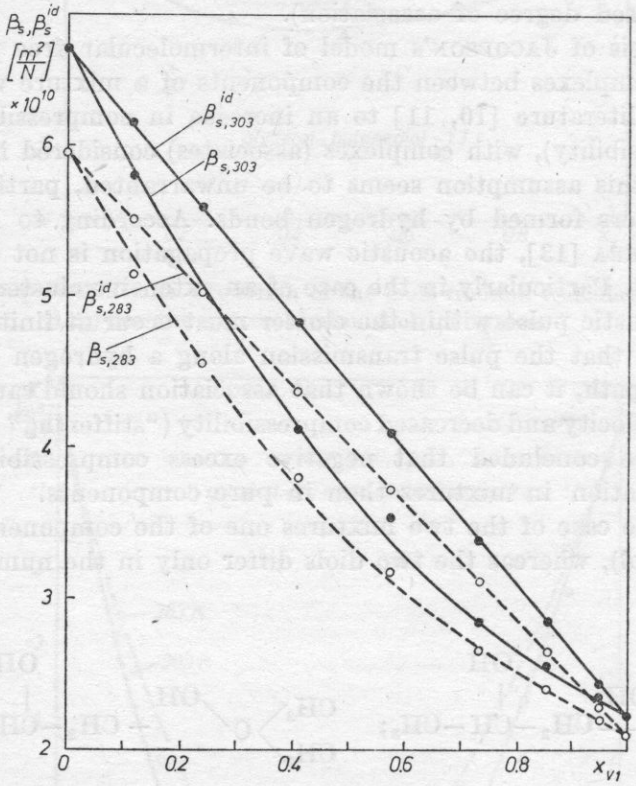

Fig. 3. The glycerol-2-methylpentanediol-2.4 system. The dependence of the coefficients of adibatic compressibility of a real mixture, β_s, and an ideal one, β_s^{id}, on the concentration, expressed in volume fractions x_{v1}, for temperatures given in the figure

ssibility of the system at the temperature T_2 is obviously greater than that at the temperature T_1 (Fig. 3).

References

[1] I. PRIROGINE, R. DEFAY, *Chemische Thermodynamik*, VES Deutscher Verlag f. Grundstoffindustrie, Leipzig 1962.

[2] L. ROTHHARDT, Z. Phys. Chem. (Leipzig), **207**, 397 (1957).

[3] I. G. MIKHAYLOV, N. A. SOLOVEV, Y. P. SYRNIKOV, *Osnovy molekularnoy akustiki*, Nauka, Moscow 1964.

[4] S. ERNST, J. GLIŃSKI, B. JEŻOWSKA-TRZEBIATOWSKA, Acta Phys. Polonica, **A55**, 501 (1979).

[5] T. A. Litowitz, R. Piccirelli, J. Acoust. Soc. Am., **29**, 1009 (1957).
[6] R. Meister, C. J. Meerhoeffer, R. Sciamanda, L. Cotter, T. A. Litowitz, J. Appl. Physics, **31**, 854 (1960).
[7] G. E. McDuffie Jr, T. A. Litowitz, J. Chem. Phys., **37**, 1699 (1962).
[8] T. A. Litowitz, G. E. McDuffie Jr, J. Chem. Phys., **39**, 726 (1963).
[9] G. Fytas, Th. Dorfmuller, Ber. Bunsenges. Chem., **85**, 1064 (1981).
[10] K. Seshadri, N. Prabhakara Rao, K. C. Ready, Z. Phys. Chem., Neue Folge, **89**, 108 (1974).
[11] K. J. Liu, J. E. Anderson, Macromolecules, **2**, 235 (1969).
[12] B. B. Kudryavtsev, G. A. Samglina, Prim. Ultrazvuk. Issl. Veshch., **28**, 101 (1963).
[13] F. Kuczera, J. Gmyrek, Arch. Akust., **7**, 283 (1972).
[14] B. Jacobson, Acta Chem. Scand., **9**, 2, 997 (1955).

Received on 25 August, 1983

ARCHIVES OF ACOUSTICS
9, 3, 363-380 (1984)

DYNAMIC AND STATIC VISCOSITY AND ELASTICITY MODULI OF BINARY MIXTURES OF POLYHYDROXYALCOHOLS

MAREK WACIŃSKI, EDWARD ZORĘBSKI, KRZYSZTOF BEBEK

Institute of Chemistry, Silesian University
(40-006 Katowice, ul. Szkolna 9)

This paper presents the results of measurements of viscosity and mechanical shear impedance, for frequencies of 0.5, 500 and 600 MHz, of liquid mixtures of glycerol-2-methylpentanediol-2.4 and glycerol-butanediol-1.3. The components of mechanical shear impedance, dynamic viscosities, relaxation times and limiting shear moduli were calculated.

This permitted the determination of the reaction of the liquids under study to shear deformation over a wide frequency range, including viscous, viscoelastic and pure elastic reactions.

1. Introduction

A large number of interesting papers have been published recently on the viscoelasticity and structural relaxation of non-polymerised liquids, both associated and non-associated [1, 2, 3].

In the case of associated liquids both the bulk and shear viscosities relax over roughly the same frequency range, i.e. the respective relaxation times are very close [4, 5], in contrast to Knesser liquids, where thermal relaxation occurs. In addition the relaxation times show approximately the same temperature dependence. It can thus be expected that the molecular mechanisms of the two processes are similar.

Since such a close relationship between the bulk and shear viscosities is characteristic of water, where the bulk viscosity must be related to the structural one, i.e. the relaxation of tensions which occur as a result of bulk and stuctural deformations, but not to temperature functions (close to 277 K the water compression is practically isothermal), it can be assumed that also in other associated liquids the bulk viscosity is related to structural changes, where hydrogen bonds break and reproduce again in the acoustic field. Ob-

viously, the viscous relaxation (where viscosity decreases as frequency increases), observed in shear impedance measurements, must be related to both the structure of the liquid and intermolecular reactions, where hydrogen bonds play the main role. Therefore the phenomena observed for bulk and structural deformations of the medium, effected by longitudinal or transverse acoustic waves, are strictly related to the structure of the liquid. Thus, any change in the thermodynamic parameters (e.g. pressure, or temperature), or change in the composition of the liquid, should be reflected not only in the viscosity, but also in the elasticity moduli and relaxation times, determined from acoustic wave propagation, and in the impedance of transverse waves.

In the present paper, the limiting shear elasticity moduli, dynamic and static viscosities, and relaxation times, were determined from shear impedance measurements in mixtures of polyhydroxyalcohols (glycerol-2-methylpentanediol-2.4 and glycerol-butanediol-1.3).

It is shown on the basis of the investigations carried out that the shear elasticity and dynamic viscosity of polyhydroxyalcohols are affected not only by intermolecular hydrogen bonds, but also by an additional factor, related to the spatial structure (the so-called steric factor).

This would suggest the usefulness of acoustical investigation methods, based on simple shear, for structural studies of liquids and liquid mixtures.

2. Measurement quantities

The investigations have shown that the viscosity of a liquid depends on the deformation frequency and is lower under the conditions of rapidly changing shear deformations than for very slow deformation. The decrease in the viscosity is accompanied by an increase in the shear elasticity of the liquid, and thus an increase in the shear modulus G. In the case of high-frequency shear strain the shear elasticity reaches a limiting value G_∞. G_∞ is a quantity related to the molecular structure of a given liquid. The reaction of the liquid to shear stress is determined acoustically by measuring the so-called characteristic shear impedance Z, which is the ratio of shear stress to acoustic velocity.

For a solid, it is a real quantity, and is

$$Z = \varrho c_T = (\varrho G)^{1/2}, \tag{1}$$

where ϱ — density of the medium, c_T — propagation velocity of transverse waves in the medium, G — shear elasticity modulus.

In the case of a viscoelastic liquid the characteristic shear impedance Z_c^* is a complex quantity, similarly to the shear elasticity modulus G^*:

$$Z_c^* = R_c + jX_c, \quad G^* = G' + jG'';$$

thus, it follows that

$$Z_c^* = (\varrho G^*)^{1/2}. \tag{2}$$

With sufficiently high measurement frequency the imaginary component of the impedance X_c is much lower than the real component R_c, and thus can be practically neglected over this range. Hence, the high-frequency shear elasticity modulus is

$$G_\infty = \frac{R_c^2}{\varrho}, \tag{3}$$

while its inverse is the shear compliance J_∞, defined as

$$J_\infty = \frac{1}{G_\infty} = \frac{\varrho}{R_c^2}. \tag{4}$$

The viscosity isotherms, calculated from the Arrhenius equation of ideal binary mixtures, can be represented in the following way:

$$\log\eta(x_2, T) = x_1 \log\eta_1(T) + x_2 \log\eta_2(T), \tag{5}$$

where $\eta_i(T)$ and x_i are respectively the viscosity and the mole fraction of a pure component.

In order to explain deviations from the additivity of viscosity as a function of composition, GRUNBERG and NISSAN's [6] modification of equation (5) was used in the form

$$\log\eta(x_2, T) = x_1 \log\eta_1(T) + x_2 \log\eta_2(T) + 2x_1 x_2 \Gamma, \tag{6}$$

where Γ is considered the measure of deviation from the ideal behaviour of binary liquid mixtures (for $\Gamma = 0$ — ideal mixture — equation (6) becomes (5)). For $\Gamma > 0$ (positive deviation from additivity) negative deviation from the Raoult law occurs, and for $\Gamma > 0$ (negative deviation from additivity) we have positive deviation from the Raoult law [7], which involves a linear dependence of the partial pressure and total pressure as a function of the mole fraction.

The value of the mean Maxwell relaxation time $\bar{\tau}_s$ is calculated in the following way:

$$\bar{\tau}_s = \frac{\eta_s}{G_\infty}, \tag{7}$$

where η_s — static viscosity (measured by the stationary method).

In turn, the dynamic viscosity is defined in the following way:

$$\eta_d = \frac{G''}{\omega}, \tag{8}$$

where ω — angular frequency ($\omega = 2\pi f$), f — frequency.

3. Experimental part

The investigations used pure butanediol-1.3 (manufactured by Koch – Light Laboratories, U.K.), pure 2-methylpentanediol-2.4 (B.D.H. Ltd., U.K.) and glycerol, pure for analysis (P.O.Ch., Gliwice, Poland). The alcohols investigated were dehydrated by boiling under reduced pressure for about 8 hours. The water content, measured by the Fischer method, did not exceed 0.35 per cent of water by weight. The alcohol solutions were prepared by the weighing method.

3.1. Static viscosity measurement

Viscosity was measured as a function of temperature with error less than 2 per cent by using the Höppler BH 2 (GDR) viscosimeter over the temperature range 263–303 K, at temperature stability of 0.05 deg.

Since both alcohols and their mixtures, *AB*-1 to *AB*-7 and *AC*-1 to *AC*-5, satisfy the dependence proposed by MEISTER [8], $\log\eta = a + bT^{-3}$ (where a and b are constants determined by the least squares method), it was used to extrapolate viscosity over the whole measurement range. The results are listed in Table 1, which also shows the correlation coefficient r, defined as

$$r = \frac{\sum_{i=1}^{n}(x_i-\bar{x})(y_i-\bar{y})}{\sqrt{\sum_{i=1}^{n}(x_i-\bar{x})^2 \sum_{i=1}^{n}(y_i-\bar{y})^2}}, \tag{9}$$

where $x_i = T_i^{-3}$, $y_1 = \log\eta_i$; $\bar{x}$ and $\bar{y}$ are the corresponding mean values.

Table 1. The temperature dependence of viscosity (T expressed in K)

Liquid	a	$b \times 10^{-7}$	Correlation coefficient
Glycerol *A*	−3.6995	9.6632	0.9998
Glycerol – Diol *B* (2-methylpentanediol-2.4)			
AB 1. x_A = 0.185	−4.4389	8.4821	0.9999
AB 2. = 0.355	−4.2686	8.7614	0.9999
AB 3. = 0.552	−4.1479	9.2125	0.9999
AB 4. = 0.704	−4.0477	9.4041	0.9998
AB 5. = 0.828	−3.9490	9.3014	0.9999
AB 6. = 0.912	−3.9034	9.5047	0.9999
AB 7. = 0.968	−3.8433	9.1510	0.9999
Glycerol – Diol *C* (Butanediol-1.3)			
AC 1. x_A = 0.295	−3.8489	7.9549	0.9998
AC 2. = 0.495	−3.8162	8.2019	1.0000
AC 3. = 0.695	−3.8205	8.5026	0.9999
AC 4. = 0.796	−3.8822	8.8223	1.0000
AC 5. = 0.898	−3.7935	9.5152	0.9998
Diol *B*	−3.9021	7.0763	0.9989
Diol *C*	−3.9602	7.3287	0.9995

3.2. Mechanical shear impedance measurements

The measurements of mechanical shear impedance were carried out:

a) at a frequency of 0.520 MHz using the devices UWE-1 and UWE-2 (built at the Institute of Fundamental Technological Research, Polish Academy of Sciences, Warsaw, Poland), over the temperature range 245–293 K. The measurement principles were described in many papers [9], the measurement error, given by the producer, is ±5 per cent. The measured dynamic viscosity, as calculated from formula (8), was given in Table 2. This table also shows the ratio of the dynamic to the static viscosity.

b) at frequencies of 500 and 650 MHz using a prototype measurement device UWE-700, built at the Department of Physical Acoustics, Institute of Fundamental Technological Research, Polish Academy of Sciences, by means of the coefficient of shear wave reflection (k) at the liquid-solid interface. The measurement error did not exceed 10 per cent.

The measurements were carried out over the temperature range 218–253 K, determined with accuracy up to 0.1 deg. The results were calculated from the relation

$$R_c = Z_q \frac{1-k}{1+k}, \tag{10}$$

where Z_q – shear impedance of a $LiNbO_3$ crystal.

After calculating the value of R_c, the limiting moduli G_∞ were determined from relation (3) and the behaviour of its change defined as a function of temperature. The results are shown in Figs. 1 and 2.

Since the temperature dependence of G_∞ was found to be linear over the elastic range, a $G_\infty = m + nT$ type equation, where m and n are constants determined by the least squares method, was used for interpolation. The results and the correlation coefficient r are listed in Table 3.

The results are also shown graphically in the form of the dependence of G_∞ on the mole fraction of glycerol (Figs. 3 and 4). Figures also show dependencies of the relaxation times τ_s on the mole fraction of glycerol for three temperatures of 233, 253 and 273 K. The mean Maxwell relaxation time was calculated from formula (7), while its values are listed in Table 2 and shown in Figs. 7 and 8.

4. Discussion of results and conclusions

The measurements carried out on the high-frequency shear moduli and viscosity permit the following conclusions to be drawn:

1. The limiting shear modulus G_∞ of glycerol is over the whole temperature range higher than that of the mixtures of 2-methylpentanediol-2.4 and butanediol-1.3 with glycerol, despite the longer and more branched (particularly

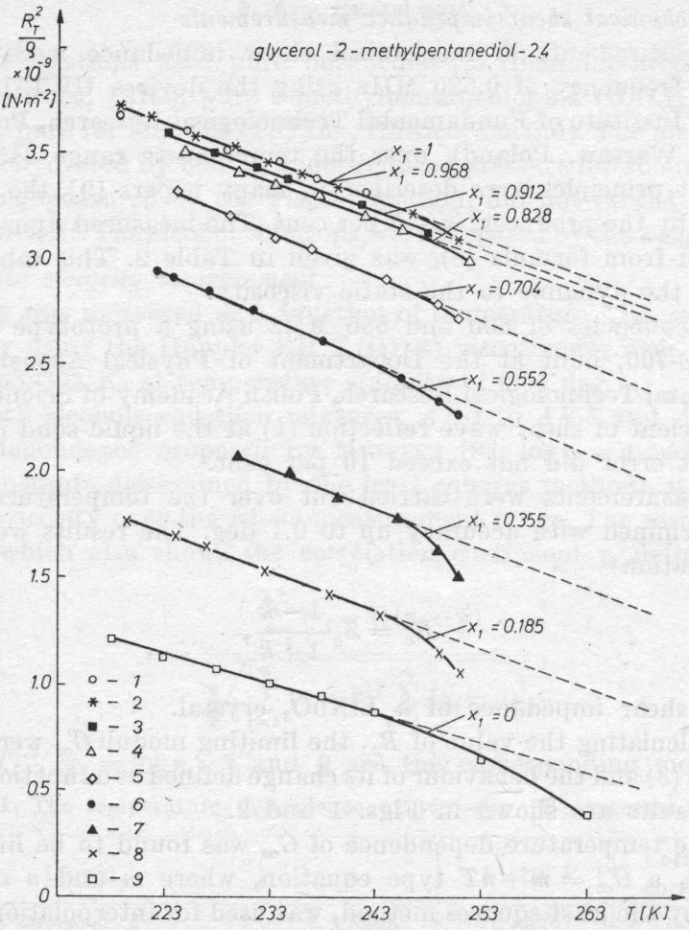

Fig. 1. The temperature dependence of the value $R_c^2 \varrho^{-1}$ and its high-frequency limiting value, G_∞, for mixtures of 2-methylpentanediol-2.4 with glycerol
1 – glycerol, *2* – AB7, *3* – AB6, *4* – AB5, *5* – AB4, *6* – AB3, *7* – AB2, *8* – AB1, *9* – diol

in 2-methylpentanediol-2.4) carbon chain of the diol. This indicates a decisive effect of intermolecular reactions (intermolecular hydrogen bonds) on the structural elasticity of alcohol in a super-cooled state.

The limiting shear modulus of the mixtures varies within the limits of the measurement error monotonously, depending on the composition of the mixture, but these changes are not a linear function of the mole fraction of the component (Figs. 3 and 4).

Over the range of low diol concentration (up to $x_{\text{diol}} = 0.2$ for 2-methylpentanediol-2.4 and up to $x_{\text{diol}} = 0.1$ for butanediol-1.3), its presence hardly affects the limiting shear modulus. The smooth, although not linear, behaviour of G_∞ as a function of the mole fraction of glycerol indicates that the elastic reaction to shear stress decreases as the cross-linking increases (i.e. with increasing density of hydroxyl groups forming hydrogen bonds).

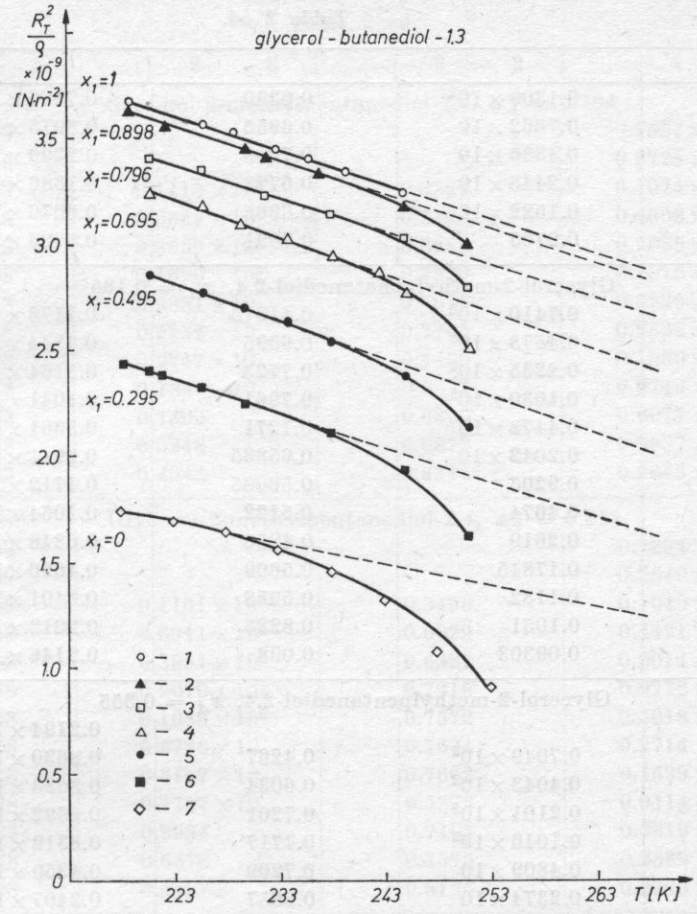

Fig. 2. The temperature dependence of the value $R_c^2 \varrho^{-1}$, and its high-frequency limiting value, G_∞, for mixtures of butanediol-1.3 with glycerol
1 – glycerol, *2* – AC5, *3* – AC4, *4* – AC3, *5* – AC2, *6* – AC1, *7* – diol

Table 2

Temp. [K]	Dynamic viscosity η_d [Nsm^{-2}]	Ratio of dynamic to static viscosities η_d/η_s	Relaxation time $\bar{\tau}_s$ [s^{-1}]
1	2	3	4
		Glycerol	
233			0.2441×10^{-5}
238			0.8476×10^{-6}
243	0.2083×10^{3}	0.1978	0.3213×10^{-6}
248	0.1244×10^{3}	0.2954	0.1318×10^{-6}
253	0.7341×10^{2}	0.4063	0.5811×10^{-7}
258	0.4128×10^{2}	0.4991	0.2734×10^{-7}
263	0.2359×10^{2}	0.58805	0.1364×10^{-7}

Table 2 cd.

1	2	3	4
268	0.1309×10^2	0.6380	0.7186×10^{-8}
273	0.7662×10	0.6955	0.3975×10^{-8}
278	0.4386×10	0.7099	0.2299×10^{-8}
283	0.2445×10	0.6778	0.1386×10^{-8}
288	0.1522×10	0.6965	0.8676×10^{-9}
293	0.9705	0.7091	0.5623×10^{-9}
	Glycerol-2-methylpenatanediol-2.4, $x_A = 0.185$		
233	0.7410×10^2	0.41315	0.1176×10^{-6}
238	0.4573×10^2	0.6595	0.4844×10^{-7}
243	0.2235×10^2	0.7723	0.2164×10^{-7}
248	0.1030×10^2	0.7961	0.1041×10^{-7}
253	0.4478×10	0.7271	0.5361×10^{-8}
258	0.2042×10	0.65835	0.2941×10^{-8}
263	0.9205	0.56005	0.1712×10^{-8}
268	0.4674	0.5122	0.1054×10^{-8}
273	0.2619	0.4956	0.6848×10^{-9}
278	0.17845	0.5609	0.4696×10^{-9}
283	0.1182	0.5958	0.3401×10^{-9}
288	0.1051	0.8225	0.2612×10^{-9}
293	0.09303	0.098	0.2146×10^{-9}
	Glycerol-2-methylpentanediol-2.4, $x_A = 0.355$		
233			0.2194×10^{-6}
238	0.7049×10^2	0.4267	0.8630×10^{-7}
243	0.4043×10^2	0.6034	0.3683×10^{-7}
248	0.2101×10^2	0.7201	0.1692×10^{-7}
253	0.1046×10^2	0.7717	0.8319×10^{-8}
258	0.4809×10	0.7209	0.4350×10^{-8}
263	0.2374×10	0.6657	0.2407×10^{-8}
268	0.1183×10	0.6276	0.1401×10^{-8}
273	0.6690	0.6237	0.8594×10^{-9}
278	0.3505	0.5520	0.5508×10^{-9}
283	0.21665	0.5557	0.3686×10^{-9}
288	0.1566	0.6331	0.2571×10^{-9}
293	0.12785	0.7898	0.1867×10^{-9}
	Glycerol-2-methylpentanediol-2.4, $x_A = 0.552$		
233			0.4858×10^{-6}
238	0.1352×10^3	0.2872	0.1802×10^{-6}
243	0.8392×10^2	0.4606	0.7276×10^{-7}
248	0.4748×10^2	0.6246	0.3172×10^{-7}
253	0.2536×10^2	0.7472	0.1483×10^{-7}
258	0.1294×10^2	0.8030	0.7387×10^{-8}
263	0.6648×10	0.8224	0.3900×10^{-8}
268	0.3435×10	0.8051	0.2171×10^{-8}
273	0.3435×10	0.71715	0.1269×10^{-8}
278	0.1691×10	0.6470	0.7764×10^{-9}
283	0.8790	0.6843	0.4954×10^{-9}
288	0.5565	0.6756	0.3287×10^{-9}
293	0.3407	0.8766	0.2264×10^{-9}

Table 2 cd.

1	2	3	4
Glycerol-2-methylpentanediol-2.4, $x_A = 0.704$			
233			0.7557×10^{-6}
238			0.2728×10^{-6}
243	0.1113×10^{3}	0.3567	0.1074×10^{-6}
248	0.6528×10^{2}	0.5108	0.4568×10^{-7}
253	0.3639×10^{2}	0.6485	0.2085×10^{-7}
258	0.1920×10^{2}	0.7322	0.1015×10^{-7}
263	0.9831×10	0.7618	0.5239×10^{-8}
268	0.5232×10	0.7745	0.2852×10^{-8}
273	0.2747×10	0.7450	0.1630×10^{-8}
278	0.1394×10	0.6635	0.9749×10^{-9}
283	0.7863	0.6320	0.6077×10^{-9}
288	0.5248	0.6872	0.3937×10^{-9}
293	0.4042	0.8344	0.2643×10^{-9}
Glycerol-2-methylpentanediol-2.4, $x_A = 0.828$			
233			0.7294×10^{-6}
238			0.2640×10^{-6}
243	0.1161×10^{3}	0.3496	0.1040×10^{-6}
248	0.6911×10^{2}	0.5029	0.4421×10^{-7}
253	0.3851×10^{2}	0.6327	0.2014×10^{-7}
258	0.2070×10^{2}	0.7216	0.9772×10^{-8}
263	0.1083×10^{2}	0.7572	0.5018×10^{-8}
268	0.5726×10	0.7634	0.2714×10^{-8}
273	0.3157×10	0.7662	0.1539×10^{-8}
278	0.1747×10	0.7396	0.9114×10^{-9}
283	0.9994	0.7103	0.5616×10^{-9}
288	0.6578	0.7575	0.3589×10^{-9}
293	0.44975	0.8125	0.2373×10^{-9}
Glycerol-2-methylpentanediol-2.4, $x_A = 0.912$			
233			0.1141×10^{-5}
238			0.4035×10^{-6}
243	0.1490×10^{3}	0.2917	0.1556×10^{-6}
248	0.8765×10^{2}	0.42275	0.6490×10^{-7}
253	0.4917×10^{2}	0.5450	0.2905×10^{-7}
258	0.2503×10^{2}	0.5983	0.1386×10^{-7}
263	0.1384×10^{2}	0.6742	0.7007×10^{-8}
268	0.7551×10	0.7111	0.3736×10^{-8}
273	0.4231×10	0.7346	0.2091×10^{-8}
278	0.2451×10	0.7518	0.1223×10^{-9}
283	0.1405×10	0.7315	0.7449×10^{-9}
288	0.8753	0.7462	0.4710×10^{-9}
293	0.6012	0.8120	0.3082×10^{-9}
Glycerol-2-methylpentanediol-2.4, $x_A = 0.968$			
233			0.6996×10^{-6}
238			0.2576×10^{-6}
243	0.1247×10^{3}	0.3746	0.1031×10^{-6}
248	0.7422×10^{2}	0.5312	0.4447×10^{-7}
253	0.4254×10^{2}	0.6782	0.2053×10^{-7}

Table 2 cd.

1	2	3	4
258	0.2174×10^2	0.7265	0.1009×10^{-7}
263	0.1209×10^2	0.8015	0.5239×10^{-8}
268	0.6495×10	0.8125	0.2864×10^{-8}
273	0.3558×10	0.8024	0.1641×10^{-8}
278	0.2066×10	0.8054	0.9808×10^{-9}
283	0.1205×10	0.7823	0.6097×10^{-9}
288	0.7817	0.8157	0.3929×10^{-9}
293	0.5231	0.8501	0.2617×10^{-9}
	2-methylpentanediol-2.4		
233	0.3359×10^2	0.6996	0.4794×10^{-7}
238	0.1770×10^2	0.8146	0.2323×10^{-7}
243	0.6731×10	0.6423	0.1206×10^{-7}
248	0.2845×10	0.5313	0.6673×10^{-8}
253	0.1306×10	0.4529	0.3916×10^{-8}
258	0.5069	0.3117	0.2428×10^{-8}
263	0.1937	0.2023	0.1587×10^{-8}
268	0.09713	0.1657	0.1091×10^{-8}
273	0.06843	0.1841	0.7894×10^{-9}
278			0.6017×10^{-9}
283			0.4817×10^{-9}
	Butanediol-1.3		
233	0.3781×10^2	0.5692	0.4130×10^{-7}
238	0.2434×10^2	0.8328	0.1870×10^{-7}
243	0.1271×10^2	0.9253	0.9052×10^{-8}
248	0.6996×10	1.020	0.4656×10^{-8}
253	0.3700×10	1.030	0.2529×10^{-8}
258	0.2199×10	1.100	0.1444×10^{-8}
263	0.1478×10	1.290	0.8629×10^{-9}
268	0.9387	1.350	0.5373×10^{-9}
273	0.5544	1.280	0.3474×10^{-9}
278	0.2999	1.070	0.2326×10^{-9}
283	0.1745	0.9410	0.1608×10^{-9}
288			0.1144×10^{-9}
293			0.8368×10^{-10}
	Glycerol-butanediol-1.3, $x_A = 0.295$		
233	0.9736×10^2	0.3636	0.1215×10^{-6}
238	0.5761×10^2	0.5246	0.5181×10^{-7}
243	0.3193×10^2	0.6599	0.2378×10^{-7}
248	0.1702×10^2	0.7484	0.1166×10^{-7}
253	0.9108×10	0.8033	0.6073×10^{-8}
258	0.4935×10	0.8283	0.3342×10^{-8}
263	0.2722×10	0.8286	0.1934×10^{-8}
268	0.1704×10	0.9011	0.1172×10^{-8}
273	0.9157	0.8079	0.7408×10^{-9}
278	0.4916	0.6981	0.4870×10^{-9}
283	0.3033	0.6708	0.3320×10^{-9}

Table 2 cd.

1	2	3	4
	Glycerol-butadienol-1.3, $x_A = 0{,}495$		
288	0.2156	0.7205	0.2342×10^{-9}
293	0.1717	0.8433	0.1700×10^{-9}
233	0.1458×10^3	0.3423	0.1717×10^{-6}
238	0.9154×10^2	0.5075	0.7104×10^{-7}
243	0.5078×10^2	0.6552	0.3170×10^{-7}
248	0.2704×10^2	0.7598	0.1514×10^{-7}
253	0.1388×10^2	0.7998	0.7695×10^{-8}
258	0.7321×10	0.8188	0.4137×10^{-8}
263	0.3972×10	0.8209	0.2342×10^{-8}
268	0.2242×10	0.8184	0.1398×10^{-8}
273	0.1260×10	0.7799	0.8605×10^{-9}
278	0.7315	0.7398	0.5547×10^{-9}
283	0.4710	0.7521	0.3710×10^{-9}
288	0.2881	0.7040	0.2568×10^{-9}
293	0.2276	0.8273	0.1835×10^{-9}
	Glycerol-butanediol-1.3, $x_A = 0.695$		
233			0.2350×10^{-6}
238	0.1255×10^3	0.4207	0.1008×10^{-6}
243	0.7218×10^2	0.5811	0.4338×10^{-7}
248	0.4186×10^2	0.7551	0.2003×10^{-7}
253	0.2347×10^2	0.8912	0.9861×10^{-8}
258	0.1193×10^2	0.9011	0.5143×10^{-8}
263	0.6258×10	0.8932	0.2827×10^{-8}
268	0.3217×10	0.8283	0.1631×10^{-8}
273	0.1734×10	0.7719	0.9831×10^{-9}
278	0.1034×10	0.7659	0.6171×10^{-9}
283	0.6931	0.8239	0.4020×10^{-9}
288	0.4199	0.7760	0.2711×10^{-9}
293	0.2982	0.8317	0.1887×10^{-9}
	Glycerol-butanediol-1.3, $x_A = 0.796$		
233			0.3697×10^{-6}
238	0.1558×10^3	0.3486	0.1411×10^{-6}
243	0.9163×10^2	0.5095	0.5836×10^{-7}
248	0.5127×10^2	0.6585	0.2595×10^{-7}
253	0.2831×10^2	0.7870	0.1232×10^{-7}
258	0.1497×10^2	0.8496	0.6209×10^{-8}
263	0.7766×10	0.8530	0.3302×10^{-8}
268	0.4000×10	0.8104	0.1845×10^{-8}
273	0.2165×10	0.7759	0.1078×10^{-8}
278	0.1335×10	0.8903	0.5663×10^{-9}
283	0.8179	0.8103	0.4149×10^{-9}
288	0.5047	0.7856	0.2715×10^{-9}
293	0.3800	0.9119	0.1835×10^{-9}
	Glycerol-butanediol-1.3, $x_A = 0.898$		
233			0.1525×10^{-5}
238			0.5383×10^{-6}
243	0.1790×10^3	0.2674	0.2072×10^{-6}

Table 2 cd.

1	2	3	4
248	0.1096×10^3	0.4040	0.8623×10^{-7}
253	0.6400×10^2	0.5391	0.3851×10^{-7}
258	0.3724×10^2	0.6817	0.1834×10^{-7}
263	0.1998×10^2	0.7453	0.9255×10^{-8}
268	0.1102×10^2	0.7954	0.4925×10^{-8}
273	0.6034×10	0.8039	0.2750×10^{-8}
278	0.3427×10	0.8070	0.1605×10^{-8}
283	0.2066×10	0.8263	0.9759×10^{-9}
288	0.1237×10	0.8104	0.6157×10^{-9}
293	0.7663	0.7959	0.4019×10^{-9}

Table 3. The temperature dependence of the limiting shear elasticity modulus $G_\infty = m + nT$ [Nm^{-2}]. Temperature in K

Liquid	$m \times 10^{-9}$	$n \times 10^{-7}$	Correlation coefficient
1	2	3	4
Glycerol *A*	7.3831	−1.6883	−0.9833
Glycerol-Diol *B* (2-methylpentanediol-2.4)			
AB 1. $x_A = 0.185$	5.9202	−1.8848	−0.9986
AB 2. $x_A = 0.355$	6.4504	−1.9046	−0.9975
AB 3. $= 0.552$	7.7481	−2.1565	−0.9991
AB 4. $= 0.704$	8.1202	−2.1449	−0.9991
AB 5. $= 0.828$	7.3807	−1.7218	−0.9987
AB 6. $= 0.912$	7.5626	−1.7603	−0.9965
AB 7. $= 0.968$	7.5043	−1.7578	−0.9980
Glycerol-Diol *C* (Butanediol-1.3)			
AC 1. $x_A = 0.295$	6.1291	−1.6837	−0.9989
AC 2. $x_A = 0.495$	7.0447	−1.8918	−0.9972
AC 3. $= 0.695$	7.5498	−1.9274	−0.9867
AC 4. $= 0.796$	7.0216	−1.6209	−0.9746
AC 5. $= 0.898$	7.2868	−1.6686	−0.9988
Diol *B*	4.0951	−1.3269	−0.9992
Diol *C*	3.7300	−0.9100	−1.000

The deviations of G_∞ from additivity with respect to the mole fraction vary for the two mixtures, depending on the temperature.

For 2-methylpentanediol-2.4 the deviation is positive over the whole concentration range with temperatures below 273 K. It reaches its maximum value for diol concentration $x_{\text{diol}} = 0.25$, i.e. for the mole ratio glycerol: diol = 3:1, suggesting particularly strong cross-linking of the mixture close to this concentration. In the case of butanediol-1.3 mixtures the deviation becomes

positive over the whole concentration only at a temperature of 223 K. At higher temperatures the sign of deviation from additivity changes.

2. Figs. 5 and 6 show the dependence of $\log \eta$ on the mole fraction of glycerol for three temperatures of 253, 273 and 283 K. The dashed line represents the behaviour of the dependence of viscosity isotherms for ideal binary mixtures.

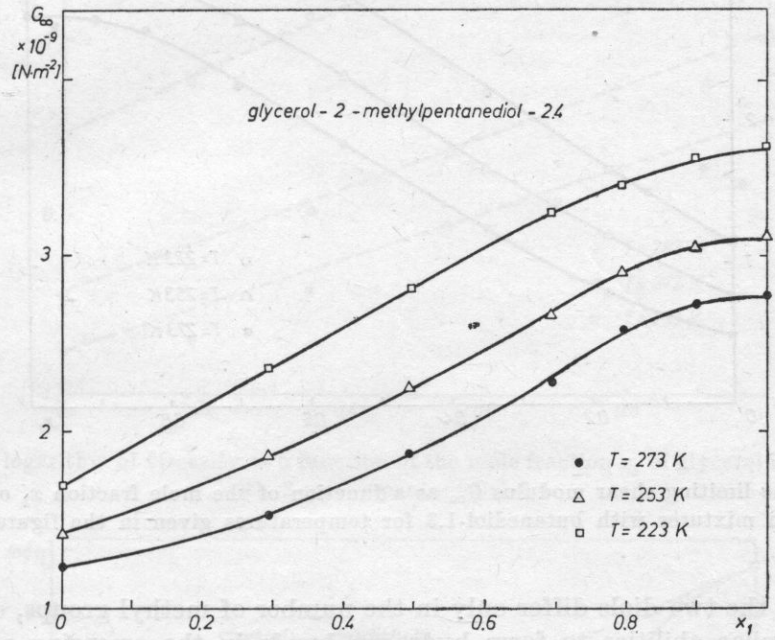

Fig. 3. The limiting shear modulus G_∞ as a function of the mole fraction x_1 of glycerol in mixtures with 2-methylpentanediol-2.4 for temperatures given in the figure

With both mixtures $\log \eta$ deviates negatively from additivity. In the case of the 2-methylpentanediol-2.4-glycerol system the deviation is particularly distinct over the diol concentration range 0.03–0.3. In this range there are also large irregularities, possibly indicating some structural peculiarities.

In contrast to 2-methylpentanediol-2.4-glycerol mixtures, in the glycerol--butanediol-1.3 system the deviation from additivity shows smooth (monotonous) behaviour, occurring over the diol concentration range 0.1–0.7, and when little more diol is added, no sharp viscosity drop results. Thus, there emerges a distinct effect of the density of OH^- groups, participating in the specific intermolecular interactions.

3. Similar deviations from additivity are characteristic of the mean relaxation time; where it is interesting to note a sharp drop in relaxation time, caused by a small addition of 2-methylpentanediol-2.4 to glycerol. This effect is not observed for mixtures of butanediol-1.3 and glycerol (Figs. 7 and 8).

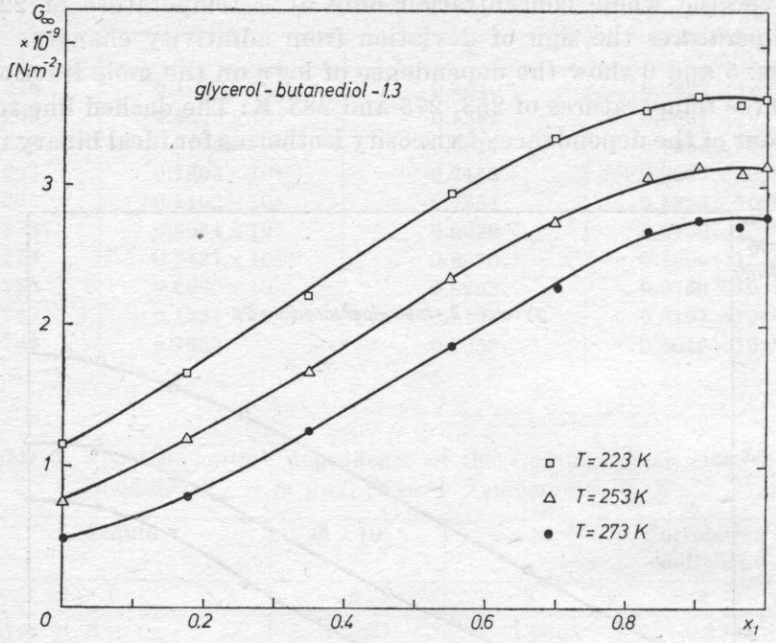

Fig. 4. The limiting shear modulus G_∞ as a function of the mole fraction x_1 of glycerol in mixtures with butanediol-1.3 for temperatures given in the figure

Since the two diols differ only in the number of methyl groups, one could expect similar abilities to form hydrogen bonds in the emerging associates, and thus similar specific intermolecular interactions leading to the formation of clusters, and determining the reaction to mechanical stress. However, 2-methylpentanediol mixtures show much greater deviation from ideality than those of butanediol-1.3 and glycerol.

It can thus be concluded that the free spaces in the openwork structure of a cluster are "blocked" by two methyl groups of 2-methylpentanediol-2.4, and that, in addition to cross-linking by hydrogen bonds, another steric factor occurs.

The results obtained indicate that peculiarities in the structure of the solutions under study are reflected in their behaviour under dynamic load. This seems to suggest the usefulness of rheological investigations based on pure stress (and thus not related to density and temperature changes) for studying the structure of liquid solutions, although it is so far impossible, in view of the necessary measurement frequency range of the order of 10^{12}–10^{13} Hz and in view of the impossibility of super-cooling over a sufficiently wide temperature range, to extend the studies to the most interesting range of aqueous solutions.

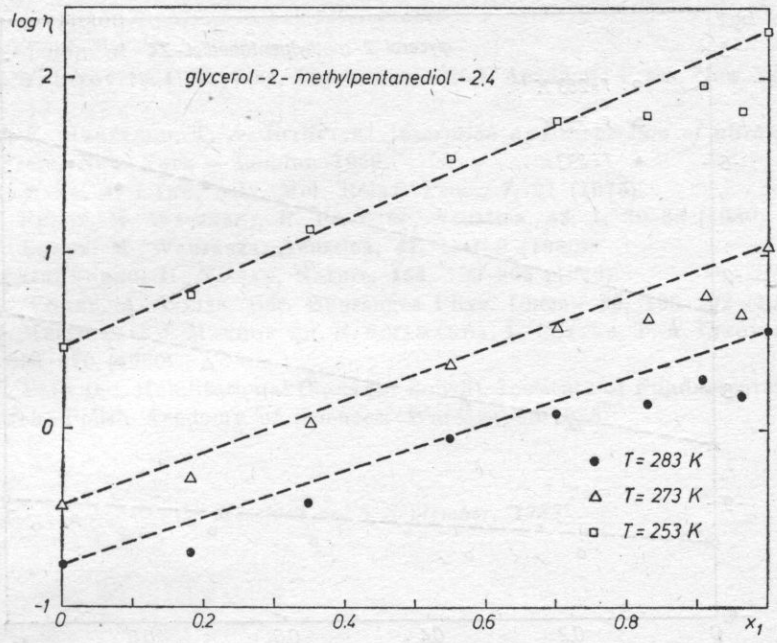

Fig. 5. The logarithm of viscosity as a function of the mole fraction x_1 of glycerol in mixtures with 2-methylpentanediol-2.4

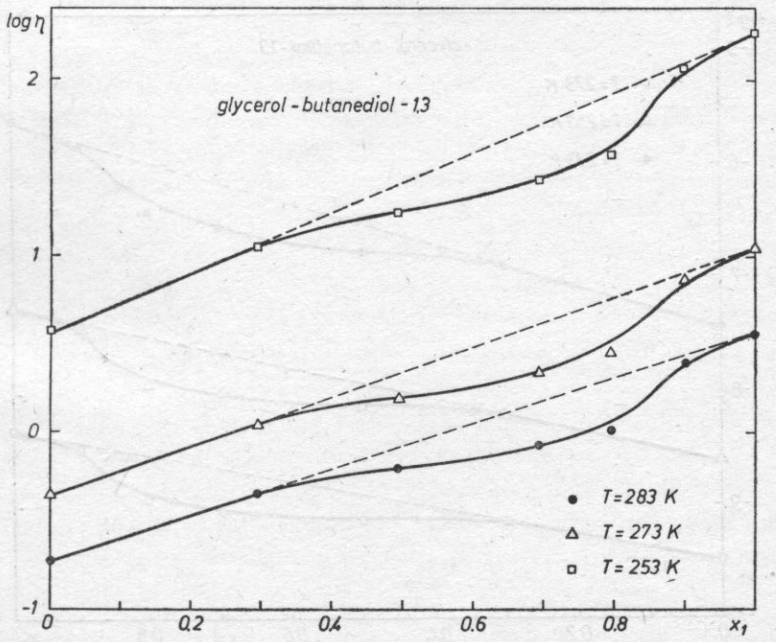

Fig. 6. The logarithm of viscosity as a function of the mole fraction x_1 of glycerol in mixtures with butanediol-1.3

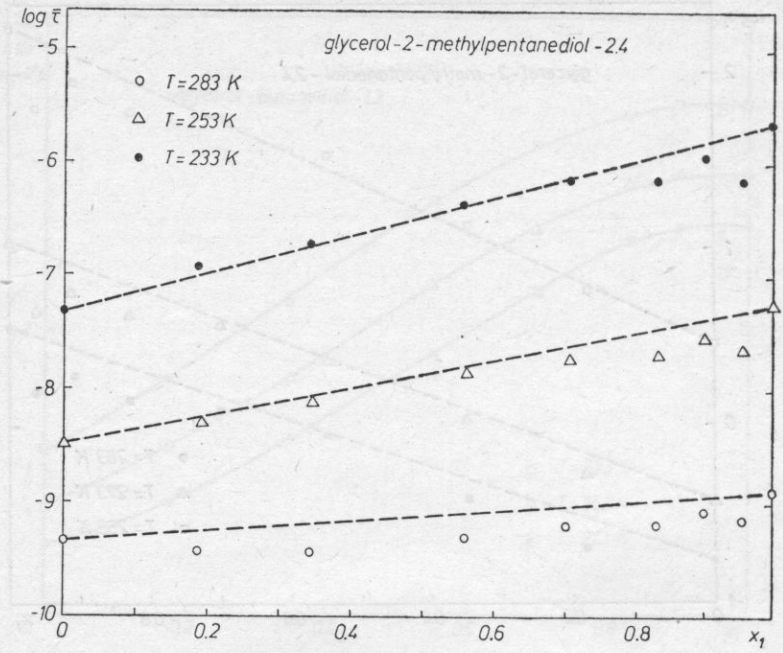

Fig. 7. The logarithm of the mean relaxation time as a function of the mole fraction x_1 of glycerol in mixtures with 2-methylpentanediol-2.4

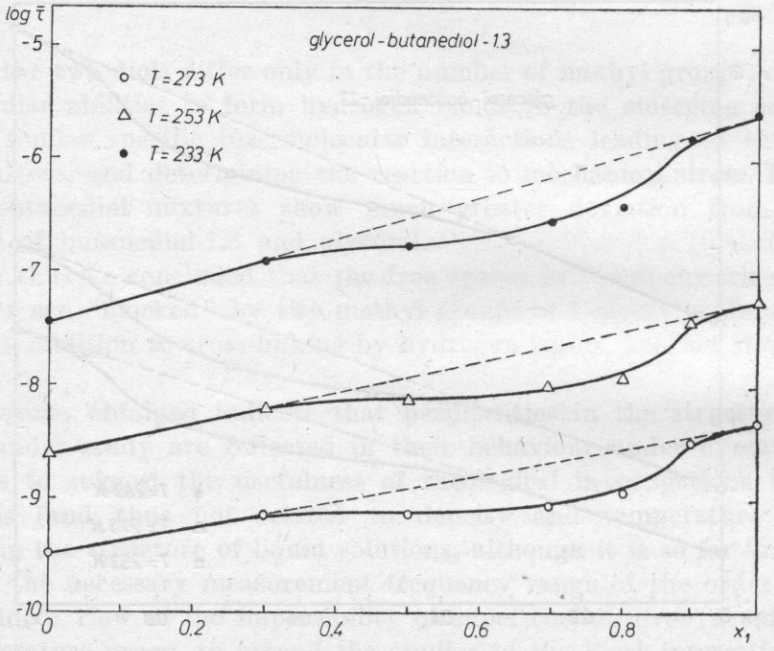

Fig. 8. The logarithm of the mean relaxation time as a function of the mole fraction in mixtures with butanediol-1.3

References

[1] T. A. LITOVITZ, C. DAVIES, *Physical acoustics*, Academic Press, New York – London 1965.

[2] K. F. HERZFELD, T. A. LITOVITZ, *Absorption and dispersion of ultrasonic waves*, Academic Press, New York – London 1959.

[3] R. ZANA, J. LANG, Adv. Mol. Relax. Proc., **7**, 21 (1975).

[4] S. ERNST, M. WACIŃSKI, R. PŁOWIEC, Acustica, **45**, 1, 30–38 (1980).

[5] S. ERNST, M. WACIŃSKI, Acustica, **47**, 1, 1–9 (1980).

[6] L. GRUNBERG, H. NISSAN, Nature, **164**, 799–805 (1949).

[7] H. VOGEL, A. WEISS, Ber. Bunsenges Phys. Chem., **86**, 193–202 (1982).

[8] R. MEISTER, C. J. MARHOFFER, R. SCIAMANDA, Ł. COTTER, T. A. LITOVITZ, J. Appl. Phys., 31, 854–870 (1960).

[9] R. PŁOWIEC, Habilitational thesis (in Polish), Institute of Fundamental Technological Research, Polish Academy of Sciences, Warsaw, 60/1975.

Received on 5 September, 1983

C H R O N I C L E

2ND SPRING SCHOOL ON ACOUSTOOPTICS AND ITS APPLICATIONS

Gdańsk-Wieżyca, 24–29 May, 1983

Three years after the 1st Spring School on Acoustooptics and its Applications (Archives of Acoustics, **16**, 3 (1981)), which had been held at Wieżyca near Gdańsk, another meeting in this field took place, organized by the Institute of Experimental Physics, Gdańsk University, in cooperation with the Section of Quantum and Molecular Acoustics and Sonochemistry of the Polish Acoustical Society and with support by the Institute of Fundamental Technological Research, Polish Academy of Sciences.

The Honorary Committee included Prof. Dr. Z. JAGODZIŃSKI, Chairman of the Polish Acoustical Society; Prof. Dr. A. KAWSKI, Deputy Rector of Gdańsk University; Prof. Dr. I. MALECKI, Institute of Fundamental Technological Research; Prof. Dr. A. OPILSKI, Chairman of the Section of Quantum and Molecular Acoustics and Sonochemistry of the Polish Acoustical Society; Prof. Dr. J. RANACHOWSKI, Institute of Fundamental Technological Research, Polish Academy of Sciences.

The Organizing Committee included Prof. Dr. A. ŚLIWIŃSKI, Chairman; Dr. A. MARKIEWICZ, Secretary; Dr. I. WOJCIECHOWSKA, Deputy Secretary; and Drs. M. BORYSEWICZ, M. KOSMOL, P. KWIEK, B. LINDE as members.

The Programme of the School consisted of physical, technical and technological problems related to interaction between light and ultrasound in fluids and solids. The points of interest were bulk, transverse and surface elastic waves interacting with a light beam, particularly a laser light beam.

Although the School took place a year later than originally planned, it lost nothing of its topical value, enjoying a large interest on the part of the experts, not only those who had participated in the 1st School in 1980, but also those who came to this working meeting for the time.

The School provided an opportunity for mutual exchange of knowledge about a large number of specific problems with which this rather narrow field of science is concerned.

70 persons took part in the School 28 lectures and original papers by invited internationally famous experts were delivered. 12 papers were presented in poster form.

The programme of the School included:

General papers

1. R. MARTENS, W. HEREMAN (Instytuut voor Theoretische Mechanica, Gent, Belgium), *Diffraction of light by ultrasonic waves in the case of oblique incidence of the light, general theory and approximations.*

2. I. Gabrielli, P. Ciuti, S. Zugna (Universite degli Studi di Trieste, Triest, Italy), *Spatial and temporal modulation of a light beam obliquelly incident on an ultrasonics beam of rectangular or circular cross-section.*
3. I. Gabrielli, P. Ciuti (Universite degli Studi di Trieste, Triest, Italy), *Light diffraction by ultrasound: analysis of special temporally modulating arrangements.*
4. K. Patorski (Warsaw Technical University, Poland), *Optical harmonic analysis of ultrasonic phase gratings — selected topics.*
5. R. Reibold (Physikalisch-Technische Bundestald, Braunschweig, FG-R), *Ultrasound investigation by laser interferometry using quadrature fringe detection.*
6. F. Michard (Universite Pierre et Marie Curie, Paris, France), *Local elastic properties investigated through acousto-optical techniques.*
7. J. Ranachowski, J. Motylewski (Institute of Fundamental Technological Research, Warsaw, Poland), *Photoacoustic spectroscopy: physical bases and preliminary research in Poland.*
8. M. Baszun (Warsaw Technical University, Poland), *A method of analysis of SAW in inhomogeneous media.*
9. P. Kwiek (Gdańsk University, Poland), *Diffraction of light by two spatially separated ultrasonic waves.*
10. A. Defebvre (Faculté Libre des Sciences, Lille, France), *Comparison between some theories of Debye-Sears phenomena.*
11. W. Hereman (Instytuut voor Technische Mechanica, Gent, Belgium), *Acousto-optic diffraction of intense laser light in an isotropic medium (including third harmonic generation).*
12. A. Milewski (Warsaw Technical University, Poland), *Optic electric and magnetic of SAW velocity.*
13. J. Kozłowski, S. Szapiel (Warsaw Technical University, Poland), *The acoustic self--stroboscopy by using an optical cyclic interferometer.*
14. A. Śliwiński (Institute of Experimental Physics, Gdańsk University, Poland), *Acousto-opitcs in anisotropic media.*
15. A. Alippi (Instituto di Acustica "O. M. Corbino", Italy), *Polarization state changes in light interaction with ultrasound.*
16. W. Pajewski (Institute of Fundamental Technological Research, Warsaw, Poland), *The influence of substrate anisotropy on diffraction focusing and reflection of a surface wave.*
17. J. Sapriel (Centre National d'Etudes de Telecommunications, France), *Lattice dynamics of acoustic modes in III–V semiconductor alloys and superlattices.*
18. A. Opilski (Silesian Technical University, Gliwice, Poland), *Technology of waveguide formation and methods of investigating waveguides applied to planar acoustooptics.*
19. A. Chyla, W. Kamiński (Aviation Institute, Warsaw, Poland), *Acoustic aspects of flow visualisation near tip of propellers and helicopter rotors.*
20. M. Szustakowski (WAT, Warsaw, Poland), *Acoustic fiber sensors.*
21. E. Danicki (PIT, Warsaw, Poland), *General theory of reflection of surface acoustic wave from periodic metal strips.*
22. G. Louis, P. Peretti (Université Pierre et Marie Curie, Paris, France), *Photoacoustic spectroscopy of organic molecules in gas phase: study in the ultraviolet and infra-red spectra.*
23. A. Komorowski, W. Zielenkiewicz (IChF, Warsaw, Poland), *Nonradiative relaxation processes in electronically excited molecule in liquid solution by photoacoustic calorimetry.*
24. L. Kovacs, Yu. V. Pisarevskii, I. M. Silvestrova (Research Laboratory for Crystals Physics, Hungarian Academy of Sciences, Budapest, Hungary), *Characterization of* TeO_2 *single crystals by the acousto-optical method.*
25. E. Kozaczka, A. Cwalina (WSM, Gdynia, Poland), *Detection and observation of propeller cavitation.*

26. S. Ait Amer, A. Benchaala, A. Dahel (City University, London, U.K.), *Visualization and metrology of ultrasonic field.*
27. J. P. Weight, A. F. Brown, S. Ait Amer (City University, London, U.K.), *High resolution ultrasonic transducer.*
28. I. Wojciechowska, A. Markiewicz (Institute of Experimental Physics, Gdańsk University, Poland), *Calculation of ultrasonic field using data obtained in holographic investigation of amplitude distribution throughout an ultrasonic transducer.*

Poster form papers

1. M. Borysewicz, A. Śliwiński (Institute of Experimental Physics, Gdańsk University, Poland), *Acoustooptic interaction in nematic liquid crystals.*
2. M. Kosmol, B. Linde, A. Śliwiński (Institute of Experimental Physics, Gdańsk, University, Poland), *Investigations of molecular processes by acoustooptical methods.*
3. A. Markiewicz (Institute of Experimental Physics, Gdańsk University, Poland), *Calculation of ultrasonic fields.*
4. J. Litniewski (Institute of Fundamental Technological Research, Warsaw, Poland), *The influence of aberration on a SAM image.*
5. I. Merta, J. Rafa (WAT, Warsaw, Poland), *Distribution of acoustic wave field in standing wave acoustooptic modulator.*
6. A. Cremisini, M. Dozio (Facolta di Ingegneria, Istituto di Matematiche Applicate U. Dinice, Pisa, Italy), *On a new algorithm describing the acoustic wave propagation.*
7. V. F. Nozdrev, S. G. Ezhov, V. A. Balanding, E. V. Gevorkijan (VZMI, Moscow, USSR), *The acoustooptical effect in nematic liquid crystals in the presence of electric field.*
8. S. Patela, J. Kądziela, J. Radojewski (WAT, Warsaw, Poland), *Acoustooptic interaction in* ZnO *waveguides on oxidized silicon substrates deposited in modified DC sputtering system.*
9. E. Soczkiewicz, *Attenuation of the mean acoustic field in random media and the form of correlation function of irregularities.*
10. O. Leroy, E. Blomme (Kortrijk, Belgium), *Double Bragg – and Bragg/Normal diffraction of two laser beams by ultrasound.*
11. O. Leroy, J. M. Claeys (Kortrijk, Belgium), *Light diffraction by one ultrasonic wave Laplace-transform method.*
12. O. Leroy, E. Blomme (Kortrijk, Belgium), *Amplitude-time-modulation of a diffracted laser beam by two ultrasonic waves with opposite directions and frequency ratio: 1 : n.*

The sessions involved numerous debates, in addition a programmatic round table discussion was held on the existing criteria permitting distinction between the Raman-Nath and Bragg ranges in the phenomenon of light diffraction by ultrasonic wave. The discussion indicated that these criteria are not sufficient and particularly unreliable in the intermediate case, i.e. in the region between those ranges, where known theories do not ensure agreement with experimental results.

The Proceedings of the 2nd School were published by Publishing Section of Gdańsk University in January 1984, as a separate collection.

The next, 3rd, School on Acoustooptics is expected take place in 1986.

Antoni Śliwiński (Gdańsk)

INFORMATION ON WINTER SCHOOLS ON MOLECULAR AND QUANTUM ACOUSTICS AND SONOCHEMISTRY AND ON VIBROACOUSTIC HAZARD CONTROL IN INDUSTRY

On 1–6 March, 1984, at Ustroń-Jaszowiec, XIIth Winter School on Molecular and Quantum Acoustics and Sonochemistry and XIth Winter School on Vibroacoustic Hazard Control in Industry were held at Ustroń-Jaszowiec, both organized by High-Silesian Division of the Polish Acoustical Society in cooperation with the Institute of Physics of Silesian Technical University.

The Organizing Committee included Dr. Joachim GMYREK (general management, programme of the School on Molecular and Quantum Acoustics and Sonochemistry), Dr. Bogusław NOSOWICZ (programme and scientific supervision of the School on Vibroacoustic Hazard Control in Industry), Zdzisław JAKUBCZYK, M.Sc. (finances), Dr. Ryszard HNATKÓW (organization), Dr. Zygmunt NICZYPORUK and Dr. Tadeusz PUSTELNY.

In the XIIth Winter School on Molecular and Quantum Acoustics and Sonochemistry, 70 participants took part. Most scientists came from the Institute of Fundamental Technological Research, Polish Academy of Science, Warsaw, Poland; WAT; and Institute of Physics of the Silesian Technical University. There were also representatives of all the scientific centres which work in this field.

In the School 47 papers and communications were delivered. Each of the 6 sessions began with a leading paper on the problems considered in a given session (acoustoelectronics, surface waves, molecular acoustics, quantum acoustics, acoustooptics, sonochemistry and ultrasonic technology). The abstracts of the papers delivered will be published in the 5th volume of the periodical "Molecular and quantum acoustics".

74 participants took part in the XIth Winter School on Vibraocoustic Hazard Control in Industry, including both employees of research and development centres, design offices and industrial plants from all over Poland. The leading problems were those related to the occurrence, measurement, analysis and evaluation of pulsed noises. A review lecture was delivered by Dr. Adam LIPOWCZAN. Another dozen-odd papers on these subjects were presented by representatives of various research institutions and industry. The other group of lectures or communications was devoted to acoustic diagnostics of industrial machinery and facilities and the broadly conceived problems related to noise control. In the School a total of 36 lectures and communications were delivered.

Joachim Gmyrek (Gliwice)

SEMINAR ON ULTRASONIC NONDESTRUCTIVE TESTING

New Delhi 5–6 December, 1983

The Seminar on Ultrasonic Nondestructive Testing was held at New Delhi on 5–6, December, 1983.

The Seminar was organized by the Ultrasonic Society of India in collaboration with the National Physical Laboratory, New Delhi. It was inaugurated by Prof. Rais AHMED, Vice-Chairman, University Grants Commission, New Delhi.

80 delegates, mostly from industries, participated. Besides 12 papers and 4 films, 5 invited lectures were arranged in the seminar over five sessions. Dr. D. SRINIVASAN, Direc-

tor, Naval Physical and Oceanographic Laboratory, Cochin, delivered his lecture on *Acoustic techniques in underwater inspection*, Dr. V. N. BINDAL, President, Ultrasonic Society of India, and Head, Material Division, NPL Delhi, talked on *Ultrasonic inspection of underwater offshore structures*, Dr. A. K. MULLICK, Joint Director, Cement Research Institute, Ballabgarh, talked on *Ultrasonic testing of concrete*, Dr. T. K. SAKSENA, Scientist, NPL, New Delhi, spoke on *The problem of calibration of probes for nondestructive testing* and Mr. J. PRASAD, Head, NDT Centre, Hindustan Aeronautics Ltd, Bangalore, talked about *Training and education programme in NDT*.

Prof. A. K. RAO, Head, Department of Aerospace Engineering, Indian Institute of Science, Bangalore, gave the key note address in the inaugural session of the Seminar and talked on *Acoustic emission*.

In this Seminar, for the first time attention was drawn to the future needs and the magnitude of the problem of underwater NDT inspection in the country. The ultrasonic nondestructive testing technique appears to be one of the most effective methods for such jobs.

In the panel discussion, various problems of utmost need were identified. These included detection and sizing of hairline crack, corrosion testing of steel embedded in concrete, induction of predetermined size cracks etc.

The panel also realized the need of developement of various types of probes for different materials such as aluminium alloys and austenitic steel welds. The panel recommended that the NPL should have all types of calibration blocks, reference standards and ultrasonic probes. It made special reference to the report of Electronics Commission, Govt. of India, published in *Electronics Information and Planning*, vol. 7, 1980, pp. 567–599. This report recommended augmentation of testing, calibration and measurement facilities for characterization and standardization of ultrasonic equipment. The panel discussion desired an early implementation of this recommendation.

V. N. Bindal (New Delhi)